Genes to Cells

Inner nuclear membrane protein Lem2 augments heterochromatin formation in response to nutritional conditions

Yoshie Tange[1,2], Yuji Chikashige[2], Shinya Takahata[3], Kei Kawakami[3], Masato Higashi[4], Chie Mori[2], Tomoko Kojidani[2,5], Yasuhiro Hirano[1], Haruhiko Asakawa[1], Yota Murakami[3]*, Tokuko Haraguchi[1,2]* and Yasushi Hiraoka[1,2]*

[1]*Graduate School of Frontier Biosciences, Osaka University, 1-3 Yamadaoka, Suita 565-0871, Japan*
[2]*Advanced ICT Research Institute Kobe, National Institute of Information and Communications Technology, 588-2 Iwaoka, Iwaoka-cho, Nishi-ku, Kobe 651-2492, Japan*
[3]*Department of Chemistry, Faculty of Science, Hokkaido University, Sapporo 060-0810, Japan*
[4]*Graduate school of Chemical Sciences and Engineering, Hokkaido University, Sapporo 060-0810, Japan*
[5]*Laboratory of Electron Microscopy, Faculty of Science, Japan Women's University, 2-8-1 Mejirodai, Bunkyo-ku, Tokyo 112-8681, Japan*

Inner nuclear membrane proteins interact with chromosomes in the nucleus and are important for chromosome activity. Lem2 and Man1 are conserved members of the LEM-domain nuclear membrane protein family. Mutations of LEM-domain proteins are associated with laminopathy, but their cellular functions remain unclear. Here, we report that Lem2 maintains genome stability in the fission yeast *Schizosaccharomyces pombe*. *S. pombe* cells disrupted for the *lem2*$^+$ gene (*lem2*Δ) showed slow growth and increased rate of the minichromosome loss. These phenotypes were prominent in the rich culture medium, but not in the minimum medium. Centromeric heterochromatin formation was augmented upon transfer to the rich medium in wild-type cells. This augmentation of heterochromatin formation was impaired in *lem2*Δ cells. Notably, *lem2*Δ cells occasionally exhibited spontaneous duplication of genome sequences flanked by the long-terminal repeats of retrotransposons. The resulting duplication of the *lnp1*$^+$ gene, which encodes an endoplasmic reticulum membrane protein, suppressed *lem2*Δ phenotypes, whereas the *lem2*Δ *lnp1*Δ double mutant showed a severe growth defect. A combination of mutations in Lem2 and Bqt4, which encodes a nuclear membrane protein that anchors telomeres to the nuclear membrane, caused synthetic lethality. These genetic interactions imply that Lem2 cooperates with the nuclear membrane protein network to regulate genome stability.

Introduction

The eukaryotic genome is organized within the nucleus, and the functional organization of the nucleus is crucial for its activities. Heterochromatin is formed preferentially beneath the nuclear envelope (reviewed in Van de Vosse *et al.* 2011; Towbin *et al.* 2013). The nuclear envelope is composed of the inner and outer nuclear membranes (INM and ONM). A number of nuclear membrane proteins have been identified in vertebrates (Schirmer *et al.* 2003; reviewed in Schirmer & Gerace 2005; Korfali *et al.* 2012). INM proteins affect spatial organization and genetic activities of chromosomes through their interaction with chromatin (reviewed in Harr *et al.* 2016). However, roles of INM proteins in chromosome functions remain to be elucidated. One of the difficulties in studying INM proteins in vertebrates arises from the fact that some of these proteins possibly share redundant functions (Liu *et al.* 2003; Huber

Communicated by: Fuyuki Ishikawa
**Correspondence:* hiraoka@fbs.osaka-u.ac.jp or yota@sci.hokudai.ac.jp or tokuko@nict.go.jp

DOI: 10.1111/gtc.12385

et al. 2009). In contrast, fungi have a relatively small number of INM proteins, which makes phenotypic assays and interpretations easier.

The fission yeast *Schizosaccharomyces pombe* has provided a striking example of nuclear reorganization, in which telomeres drastically change their positions within the nucleus through the interaction with INM proteins. In *S. pombe*, centromeres are clustered at the spindle pole body (SPB) in vegetative cells, whereas telomeres become clustered at the SPB in meiotic prophase (Chikashige *et al.* 1994). *S. pombe* Sad1 plays a key role in this process. Sad1 is a founding member of the SUN-domain (Sad1 and Unc-84) family of conserved INM proteins (Hagan & Yanagida 1995; Malone *et al.* 1999; reviewed in Hiraoka & Dernburg 2009). SUN-domain proteins form a complex with KASH-domain proteins (Klarsicht/ANC-1/Syne homology), a group of conserved ONM proteins. The SUN–KASH protein complex, also referred to as LINC (linker of nucleoskeleton and cytoskeleton) complex, plays a role in connecting the nucleus to the cytoskeleton (reviewed in Tzur *et al.* 2006; Mekhail & Moazed 2010). It has been shown that the SUN–KASH protein complex (the Sad1-Kms1 complex in *S. pombe*) plays an active role in moving chromosomes along the nuclear envelope through the interaction with telomeres (Chikashige *et al.* 2006; reviewed in Chikashige *et al.* 2007; Hiraoka & Dernburg 2009). In vegetative cells of *S. pombe*, telomeres are anchored to the nuclear membranes through the interaction between the telomere protein Rap1 and INM protein Bqt4 (Chikashige *et al.* 2009). While entering meiosis, telomeres become connected to the SPB/INM protein Sad1 through the meiosis-specific proteins Bqt1 and Bqt2, which bridge Rap1 and Sad1. Telomeres associated with the Sad1–Kms1 complex are tethered to the SPB by the dynein microtubule motor protein (Chikashige *et al.* 2006; reviewed in Chikashige *et al.* 2007; Hiraoka & Dernburg 2009). This provides a clear example of the effect of INM proteins on the chromosome organization within the nucleus.

Ima1, Lem2 and Man1 are other INM proteins identified in *S. pombe* (Hiraoka *et al.* 2011; Gonzalez *et al.* 2012; Steglich *et al.* 2012). *S. pombe* Ima1 is a homologue of the human Samp1 and rat NET5 proteins (Schirmer *et al.* 2003; Schirmer & Gerace 2005; Buch *et al.* 2009), but no obvious homologues to these mammalian proteins have been identified in the budding yeast *Saccharomyces cerevisiae*. Lem2 and Man1 belong to the conserved LEM-domain INM protein family characterized by the presence of the LEM domain of approximately 40 amino acid residues shared by its metazoan founding members (Lap2, Emerin and Man1) at the N-terminal nucleoplasmic region (Lin *et al.* 2000; Laguri *et al.* 2001; Brachner *et al.* 2005; Ulbert *et al.* 2006; Huber *et al.* 2009). In metazoans, the conserved LEM-domain protein family consists of LAP2, emerin, Man1, Lem2 (NET25), Lem3, Lem4 and Lem5 (reviewed in Lee & Wilson 2004; Gruenbaum *et al.* 2005; Wagner & Krohne 2007; Brachner & Foisner 2011; Barton *et al.* 2015). Among them, emerin is known to be mutated in a human disease called laminopathy (Bione *et al.* 1994; Yorifuji *et al.* 1997; reviewed in Berk *et al.* 2013; Worman & Schirmer 2015). Heh1 (also called Src1) and Heh2, identified in *S. cerevisiae* (King *et al.* 2006; Grund *et al.* 2008), contain the LEM-like domain called HEH (helix-extension-helix) domain (Mans *et al.* 2004; Brachner & Foisner 2011). *S. cerevisiae* Heh1 and Heh2 also contain the MSC (MAN1/Src1C-terminal) domain in the C-terminal region, which is homologous to a similar domain present in metazoan Lem2 and Man1 proteins (Mans *et al.* 2004; Brachner & Foisner 2011). *S. pombe* Lem2 and Man1 share a similar domain structure containing the HEH/LEM and MSC domains and two transmembrane domains (Hiraoka *et al.* 2011; Gonzalez *et al.* 2012; Steglich *et al.* 2012; Barrales *et al.* 2016). Chromatin is anchored to the nuclear periphery through the HEH/LEM domain (Gonzalez *et al.* 2012).

In *S. pombe*, it has been shown that Lem2, Man1 and Ima1 are localized in the nuclear envelope (Hiraoka *et al.* 2011; Gonzalez *et al.* 2012; Steglich *et al.* 2012). These three proteins apparently share redundant roles, at least in mitotic cell growth, because a loss of any one of these proteins shows no obvious defects, whereas a loss of all three proteins impairs viability (Hiraoka *et al.* 2011). However, in the present study, we found a distinct role for Lem2, as depletion of this protein, but not of Man1 or Ima1, led to increase in the minichromosome loss and defects in heterochromatin formation in response to changes in nutritional conditions.

Results

Lem2 and Man1 are conserved inner nuclear membrane proteins

Schizosaccharomyces pombe Lem2, Man1 and Ima1 have been shown as nuclear membrane proteins by fluorescence microscopy (King *et al.* 2008; Hiraoka *et al.* 2011; Gonzalez *et al.* 2012; Steglich *et al.* 2012). In addition, the N-terminus of the Ima1 protein was

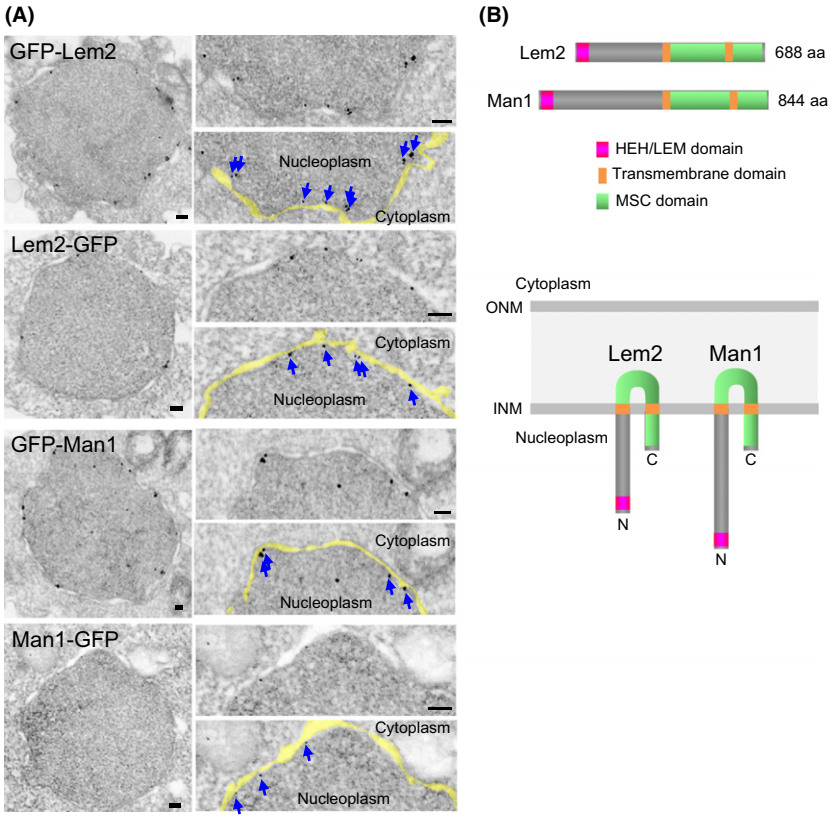

Figure 1 Immuno-electron microscopy of Lem2 and Man1. (A) Immuno-electron micrographs of N- or C-terminally tagged Lem2 (GFP-Lem2 or Lem2-GFP, respectively) and N- or C-terminally tagged Man1 (GFP-Man1 or Man1-GFP, respectively) in *Schizosaccharomyces pombe* cells. N- and C-termini tagged with GFP were detected with an anti-GFP antibody and a secondary antibody doubly conjugated with a fluorescent dye and 1.4-nm colloidal gold particles. Colloidal gold particles were enlarged by the silver enhancement treatment. Magnified images are shown in the right panels together with the color-superimposed images: yellow shades indicate the nuclear membrane; arrows indicate positions of colloidal gold particles. Bars represent 100 nm. (B) Structure of the Lem2 and Man1 proteins. Upper panel: domain structures of Lem2 and Man1. Lower panel: topology of *S. pombe* Lem2 and Man1 in the nuclear membranes according to the results of the present study.

detected at the nucleoplasmic side by immuno-electron microscopy, indicating that Ima1 is an inner nuclear membrane protein (King *et al.* 2008). To establish detailed topologies of Lem2 and Man1 in the nuclear envelope, which had not been experimentally determined in *S. pombe* previously, we detected Lem2 and Man1 by immuno-electron microscopy. Cells expressing GFP-tagged Lem2 or Man1 at the N- or C-terminus were chemically fixed and analyzed by pre-embedding methods using an anti-GFP antibody as a primary antibody (see Experimental procedures). Both GFP-tagged N- and C-terminal regions of Lem2 and Man1 were detected beneath the INM (Fig. 1A). Thus, *S. pombe* Lem2 and Man1 are INM proteins with both N- and C-termini facing toward the nucleoplasm (Fig. 1B).

Figure 2 Phenotypes of *lem2*Δ cells. (A) Loss of minichromomosomes. Colonies of wild-type (YT694), *ima1*Δ (YT2205), *man1*Δ (YT2207) and *lem2*Δ (YT2212) strains were grown on YE plates at 30 °C for 4 days. (B) Comparison of colony sizes between the wild-type (YT694) and *lem2*Δ (YT2212) strains. Colonies were grown on YE plates at 30 °C for the indicated number of days. Upper panels show colonies on 9-cm culture dishes; lower panels show magnified views of the square areas of the upper panels. (C) Growth curve of the wild-type (YT2414) and *lem2*Δ (YT2416) cells. Strains precultured in the liquid EMMG medium were transferred to the fresh liquid YE or EMMG media and cultured at 30 °C. Cells were counted at each time point indicated on the *x*-axis. The time of transfer is indicated as 0 h. (D) Minichromosome stability in the *lem2*Δ *csi1*Δ double mutant. Colonies of *lem2*Δ (YT2384), *csi1Δ* (YT2385) and *lem2*Δ *csi1Δ* (YT2386) strains were grown on YE or EMMG plates at 30 °C for 4 days.

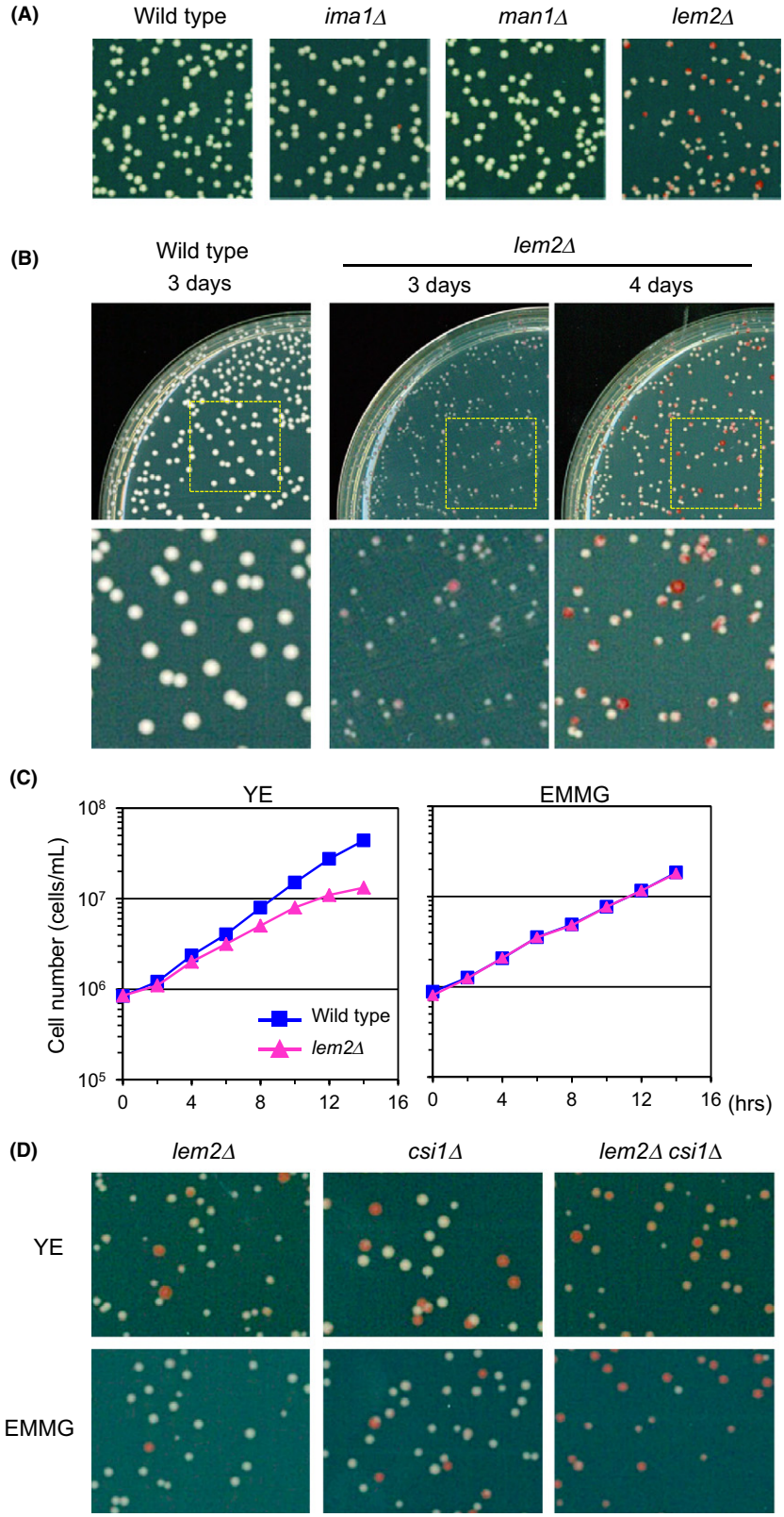

Minichromosome loss and slow growth in *lem2*Δ cells

To examine whether the INM proteins Lem2, Man1 and Ima1 affect chromosomal functions, we examined the stability of minichromosomes in mutant strains that lacked either of these proteins. We measured rates of minichromosome loss in *S. pombe* cells using the half-sector assay (Javerzat *et al.* 1996). In this assay, a minichromosome bearing the *ade6-216* allele is introduced to cells bearing the *ade6-210* allele. Cells carrying the minichromosome (*ade*$^+$) produce white colonies, whereas cells lacking the minichromosome (*ade*$^-$) produce red colonies. Thus, a colony with a red-white half sector indicates that the parental cell lost the minichromosome during the first cell division on the plate (see Experimental procedures for details).

Figure 2A shows colonies formed on the YE plate by the wild-type and mutant strains. Cells disrupted for the *lem2*$^+$ gene (*lem2*Δ) had a relatively large number of red-white half-sector colonies (9.7%) indicating a high rate of minichromosome loss (Fig. 2A; Table 1). In contrast, cells lacking the *man1*$^+$ gene (*man1*Δ) or the *ima1*$^+$ gene (*ima1*Δ) showed loss rates of 0.027% and 0.046%, respectively, only slightly higher than the loss rate of 0.012% observed in wild-type cells (Fig. 2A; Table 1). These results indicate that minichromosomes were frequently lost specifically in the absence of Lem2 and that this defect was not compensated by the presence of Man1 or Ima1. This phenotype of the minichromosome loss in *lem2*Δ cells was prominent in the rich YE medium (9.2% compared with 0.012% in wild-type cells), but moderate in the minimum EMMG medium (0.054% compared with 0.0074% in wild-type cells) (Table 1). Therefore, minichromosome stability in *lem2*Δ cells depends on the nutritional properties of the culture medium.

Table 1 Minichromosome loss rate in *lem2Δ*

Genotype	Strain name	Minichromosome loss rate (%)	
		YE	EMMG
Wild type	YT694	0.012 (8/66480)	0.0074 (5/68000)
lem2Δ	YT2212	9.2 (42/458)	0.054 (32/59420)
ima1Δ	YT2205	0.046 (35/76080)	NA
man1Δ	YT2207	0.027 (17/62640)	NA

Numbers indicate minichromosome loss rates measured by a half-sector assay in YE and EMMG.

We also investigated vegetative cell growth of *lem2*Δ cells and found that *lem2*Δ cells displayed a slow growth phenotype as they formed smaller colonies on YE plates than wild-type cells (compare wild type and *lem2*Δ at the '3 days' point in Fig. 2B). The slow growth phenotype of *lem2*Δ cells was also illustrated by the growth curves. This phenotype was obvious in the rich YE medium, but not in the synthetic minimum EMMG medium (Fig. 2C). These results indicate that defects in *lem2*Δ cells depend on nutritional conditions.

The slow growth phenotype of *lem2*Δ cells was more prominent when the cells had a minichromosome. Mutant *lem2*Δ cells bearing a minichromosome, which are distinguished by white colonies, formed smaller colonies on YE plates than wild-type cells (compare wild type and *lem2*Δ at the '3 days' point in Fig. 2B). The *lem2*Δ cells that had lost minichromosomes, which are distinguished by red colonies, grew faster than the white ones (compare '3 days' with '4 days' for *lem2*Δ in Fig. 2B), indicating that the loss of minichromosomes accelerated *lem2*Δ cell growth. This phenomenon can also contribute to a possible overestimation of half-sector colonies because red colonies become prominent when minichromosomes are lost.

Phenotypes of *lem2*Δ are distinct from phenotypes of *csi1*Δ

It has been reported that cells lacking Csi1 (*csi1*Δ), which is necessary for clustering centromeres to the SPB, show a high rate of minichromosome loss (Hou *et al.* 2012). Thus, in order to examine the genetic interaction between Lem2 and Csi1, we compared phenotypes of *lem2*Δ, *csi1*Δ and the *lem2*Δ *csi1*Δ double mutant. Phenotypes of *csi1*Δ were distinct from those of *lem2*Δ. In *csi1*Δ cells, minichromosome loss was independent of nutritional conditions, as red and red-white colonies occurred in both the rich YE medium and the minimum EMMG medium (Fig. 2D). In addition, *csi1*Δ cells formed red and white colonies of a similar size (Fig. 2D), indicating that cell growth was not affected by the presence of minichromosomes. This was in contrast to observations in the *lem2*Δ mutant as red colonies were larger than white ones (Fig. 2B,D): *lem2*Δ cells with a minichromosome (white colony) showed more severe growth defects than those without it (red colony). Finally, a larger number of red and red-white *lem2*Δ *csi1*Δ colonies indicated that the minichromosome loss was more severe in the double mutant than in

either of the single mutants (Fig. 2D). These results suggest that effects of Lem2 and Csi1 on minichromosome stability are additive and that these proteins likely function in separate pathways.

Defective heterochromatin formation in *lem2*Δ cells

Because the high rate of the minichromosome loss suggested that segregation of chromosomes was impaired in the absence of Lem2, we examined whether Lem2 is associated with centromere structures. We first examined localization of Lem2 on the centromeric sequences by chromatin immunoprecipitation (ChIP) in cells cultured in YES. We found that Lem2 was localized to the central core region of the centromere, but not outside it (Fig. 3A,B). Specifically, localization of Lem2 was restricted to the *cnt* region and a portion of the *imr* region, that is, the so-called CENP-A chromatin characterized by the presence of the CENP-A protein.

We next examined centromeric heterochromatin formation using ChIP with specific antibodies against the dimethylated form of histone H3 at the lysine 9 residue (H3K9me2) that is characteristic of heterochromatin at outer centromere regions. We found that the level of H3K9me2 was reduced in *lem2*Δ cells at the heterochromatic *dg* and *dh* repeats as well as at the marker gene inserted in heterochromatin (*imr::ura4*) (Fig. 3C). This indicated that centromeric heterochromatin was defective in the absence of Lem2. We confirmed that localization of histone H3 and CENP-A (Cnp1) at the centromere was unchanged by the depletion of Lem2 despite Lem2 co-localized with CENP-A chromatin (Fig. 3D).

In *S. pombe*, centromeric heterochromatin is formed in separate, RNA interference (RNAi)-dependent and RNAi-independent pathways. The latter pathway depends on the histone deacetylase Sir2 and heterochromatin protein Swi6 (Alper *et al.* 2012; Buscaino *et al.* 2013). Heterochromatin formed at the *dg* and *dh* centromeric repeats depends on both pathways, whereas heterochromatin formed at the marker gene inserted at *imr* depends only on the RNAi-dependent pathway. This conclusion was drawn from a complete absence of H3K9me2 at *imr::ura4* and presence of residual H3K9me2 at *dh* and *dg* in cells lacking *dcr1*, which is essential for RNAi (Fig. 3C). A moderate amount of H3K9me2 is retained at *imr::ura4,* and this methylation was almost completely prevented in the *lem2*Δ*dcr1*Δ double mutant (Fig. 3C). Moreover, although residual amounts of H3K9me2 at the *dg* and *dh* repeats could be observed in *lem2*Δ and *dcr1*Δ cells, the H3K9me2 level was even lower ($P < 0.001$; two-sided Student's *t*-test) in *lem2*Δ*dcr1*Δ cells (Fig. 3C). These results indicated that Lem2 takes part in the centromeric heterochromatin formation mainly via the RNAi-independent pathway.

The *lem2*Δ phenotypes of slow growth and minichromosome loss were observed in the rich YES medium but not in the minimum EMMG medium. These results prompted us to examine H3K9me2 levels after cells grown in EMMG were transferred to YES. H3K9me2 levels in wild-type cells became gradually higher at the outer regions of the centromere (*imr195*, *dg* and *dh* in Fig. 3A) for 12 h in the YES medium (Fig. 4A). Interestingly, this increase was considerably reduced in *lem2*Δ cells (Fig. 4A). These results suggest that centromeric heterochromatin formation was augmented after the transfer from the minimum to the rich medium. Furthermore, we found that localization of Lem2 at CENP-A chromatin occurred only in the YES medium but not in the EMMG medium (Fig. 4B), whereas protein levels of Lem2 as measured by Western blotting showed no obvious differences in either of the culture media (Fig. 4C). Thus, the augmentation of centromeric heterochromatin formation was mediated by the nutrition-dependent localization of Lem2 at CENP-A chromatin.

Suppressors of *lem2*Δ cells

Suppressors of *lem2*Δ cells were obtained spontaneously during culturing *lem2*Δ cells on YE plates. Although *lem2*Δ cells typically showed a slow growth phenotype on YE plates and formed colonies smaller than those of wild-type cells, we noticed that large colonies occasionally appeared among the predominantly small *lem2*Δ colonies (Fig. 5A). Results of the half-sector assay (Table 2) indicated that the minichromosome loss was also rescued in these suppressors (*lem2*Δ $sup^{lem2\Delta}$). We picked large colonies and carried out their genetic analysis. In the tetrad analysis, after crossing with a wild-type cell, the phenotype of the suppressor that formed large colonies on the background of *lem2*Δ showed 2 : 2 segregation. This indicated that the phenotype was linked to a single gene locus. Then, we chose a tetratype tetrad (a tetrad containing four different genotypes) and determined the whole-genome sequence in each of the tetrad progenies to search for mutations associated with the large and small colony size. We failed to

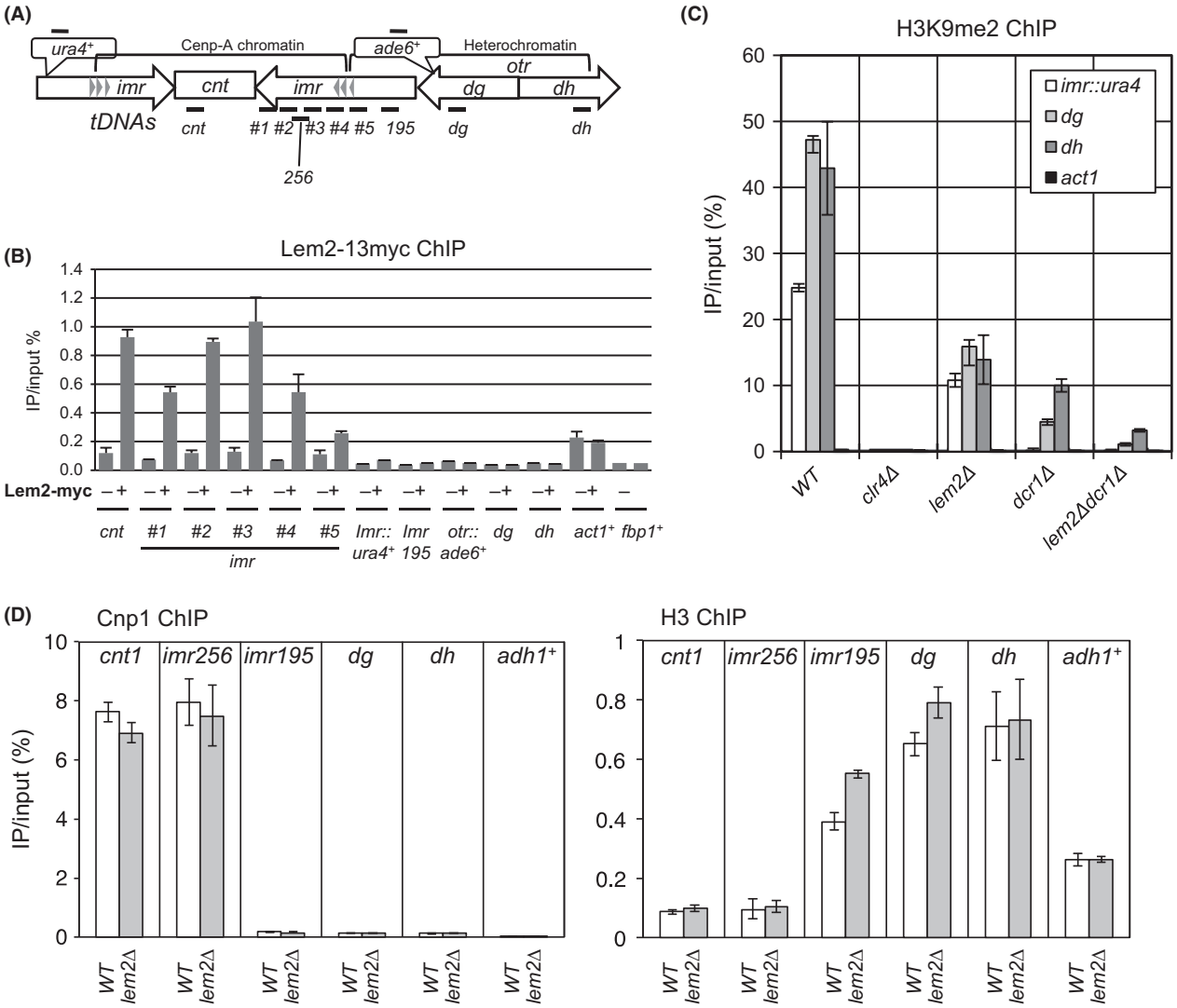

Figure 3 Defective centromeric heterochromatin in *lem2*Δ cells. (A) Schematic representation of centromere 1. The positions of the inserted marker genes (*imr1L::ura4*$^+$ and *otr1R:: ade6*$^+$) in the strain used in the panels B, C, and D are shown. Gray triangles in the *imr* region represent the cluster of tRNA genes (*tDNAs)* that forms a boundary between heterochromatin and CENP-A chromatin. Black bars indicate the positions of the PCR products in chromatin immunoprecipitation (ChIP) assay. (B) Localization of Lem2 at the center region of the centromere. ChIP analysis of Lem2-13myc at the indicated centromeric loci in cells expressing Lem2-13myc and in control cells. The ratios of immunoprecipitated DNA to input DNA are indicated. (C) ChIP analysis of H3K9me2 at the indicated loci in the indicated strains. The ratios of immunoprecipitated DNA to input DNA are indicated. (D) ChIP analyses of Cnp1 (left) and histone H3 (right) at the indicated loci in wild-type and *lem2*Δ cells. The ratios of immunoprecipitated DNA to input DNA are indicated. ChIP analyses in (B–D) were carried out in cells cultured in YES.

detect any base substitutions linked to the phenotype in protein coding and promoter regions, but found that the number of reads of a 40-kb region on chromosome III was twice larger in the *lem2*Δ *sup*$^{lem2\Delta}$ than in *lem2*Δ (Fig. 5B), suggesting that a duplication of that sequence complemented the small colony phenotype of *lem2*Δ cells.

Interestingly, this 40-kb duplicated region was flanked by the long-terminal repeat (LTR) sequences of retrotransposons at both ends (Fig. 5B). Three LTR sequences with nucleotide identity over 95% in the same direction were annotated in this 40-kb region (LTR1, LTR2 and LTR3 in Fig. 5B). By analyzing genomic DNA of the *lem2*Δ *sup*$^{lem2\Delta}$ strain

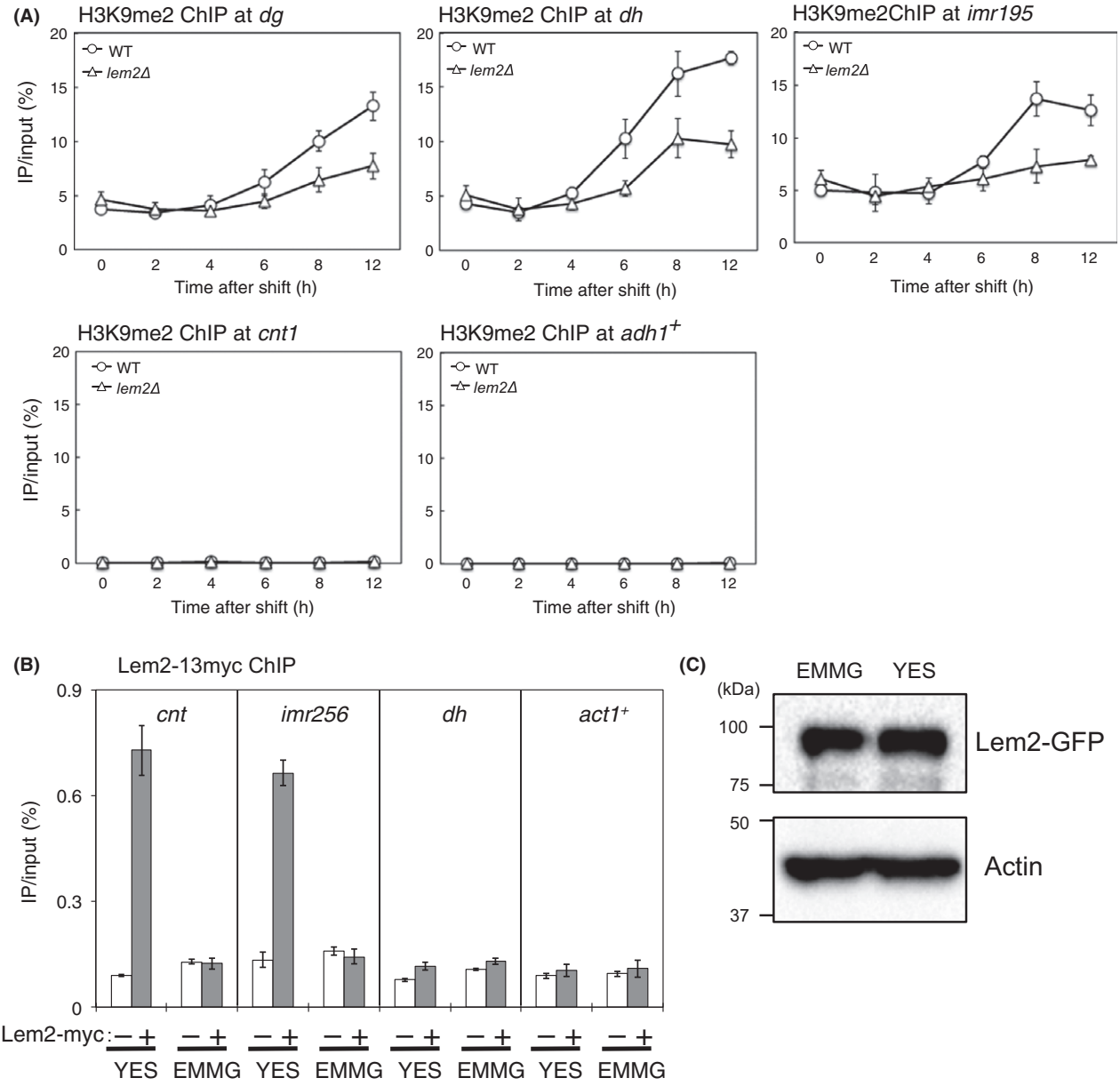

Figure 4 Nutrition-dependent accumulation of Lem2 and H3K9me2 at the centromere. (A) Time course of H3K9me2 changes at the indicated loci showed by chromatin immunoprecipitation (ChIP) experiments in wild-type and *lem2*Δ cells. Cells were first cultured in the EMMG media and transferred into the YES media at time 0. Samples were collected at indicated time points, and ChIP assays were carried out. The ratios of immunoprecipitated DNA to input DNA are indicated. (B) Centromere localization of Lem2. The localization of Lem2 at the center region of the centromere was affected by the nutritional conditions. Lem2-13myc ChIP analysis was carried out at the indicated loci in cells expressing Lem2-13myc and in no-tag control cells grown in YES or EMMG medium. Relative ratios of immunoprecipitated DNA to input DNA are indicated. (C) Expression levels of Lem2. The protein amount of Lem2-GFP under YES and EMMG media was examined by Western blot.

using PCR, we detected a PCR product that was expected to be generated if duplication occurred by recombination between the LTR1 and LTR3 sequences: nucleotide sequences determined for the PCR product confirmed the presence of the recombined LTR3–LTR1 sequences (Fig. 5C,D). We isolated 15 additional suppressor strains of *lem2*Δ and analyzed their genomic DNA by PCR in an attempt

Figure 5 Suppressors of Lem2 depletion. (A) Suppression of the small colony size phenotype in *lem2*Δ by the suppressor mutation. Strains of indicated genotypes were inoculated on the YE plate media and incubated at 30 °C for 2 days. The following strains were used: wild type (YT2414), $sup^{lem2\Delta}$ (YT2567), *lem2*Δ (YT2416) and *lem2*Δ $sup^{lem2\Delta}$ (YT2566). (B) Overlap of the long-terminal repeat (LTR)-flanked region of chromosome III in a $sup^{lem2\Delta}$ strain. The number of reads at the indicated region of chromosome III in the *lem2*Δ (YT2565) and *lem2*Δ $sup^{lem2\Delta}$ (YT2566) strains was plotted as normalized values of the number of reads in a wild-type strain (YT2568) according to the results of whole-genome sequencing analysis. Blue arrowheads indicate positions and directions of the LTR sequences (LTR1, LTR2 and LTR3). (C) Schematic diagrams of the genome structure between LTR1 and LTR3 in the wild-type (upper) and $sup^{lem2\Delta}$ (lower) strains. Blue arrowheads indicate positions and directions of the LTR sequences. Magenta arrows indicate positions and directions of PCR primers used for amplification of the fused regions. (D) Recombination between LTR1 and LTR3 in the $sup^{lem2\Delta}$ strain. Upper panel—a schematic diagram of the recombined region amplified by the specific PCR primers. Thick line represents the LTR sequence; thin line represents a flanking sequence of LTR1 or LTR3. Lower panel—nucleotide sequences of the recombined region in the chromosome III of the $sup^{lem2\Delta}$ strain. Red letters represent the LTR sequence. The region highlighted in yellow represents sequences specific to LTR3 and its flanking region. The region highlighted in blue represents sequences specific to LTR1 and its flanking region. The region highlighted in green represents overlapping sequences common in LTR1 and LTR3. (E) Summary of obtained suppressor mutants. (F) Recombination between LTR2 and LTR3 in suppressor strains. Upper panel—a schematic diagram of the recombined region amplified by the specific PCR primers. Thick line represents the LTR sequence; thin line represents a flanking sequence of LTR2 or LTR3. Lower panel—nucleotide sequences of the recombined region in chromosome III of the $sup^{lem2\Delta}$ strain. Red letters represent the LTR sequence. The region highlighted in yellow represents sequences specific to LTR3 and its flanking region. The region highlighted in blue represents sequences specific to LTR2 and its flanking region. The region highlighted in green represents overlapping sequences common in LTR2 and LTR3. In these strains, the potential recombined region includes the full length of the LTR2 sequence.

to detect recombination between LTR1, LTR2 and LTR3 sequences. Among these 15 suppressor strains, four strains possessed the recombined LTR3–LTR1 sequences identified in the initial suppressor strain that contained the 40-kb duplication and six strains had recombined LTR3–LTR2 sequences that were caused by a duplication of 10-kb sequences between LTR2 and LTR3 (Fig. 5E,F). Thus, we concluded that the small colony phenotype of *lem2*Δ cells was suppressed by the duplication of 10-kb sequences flanked by LTR2 and LTR3.

Duplication of the *lnp1*$^+$ gene suppresses *lem2*Δ phenotypes

The region between LTR2 and LTR3 on chromosome III harbors six genes (Fig. 6A). We further narrowed the chromosome region responsible for the suppressor phenotype by integrating an extra copy of each of these genes at the *lys1* site and found that a duplication of a single ORF was sufficient to suppress the slow growth phenotype of *lem2*Δ cells (Fig. 6B). This ORF encodes a homologue of the human Lunapark protein; thus, we named this gene *lnp1*$^+$. Lnp1/Lunapark is an endoplasmic reticulum (ER) membrane protein conserved in yeast (Chen *et al.* 2012) and mammals (Spitz *et al.* 2003). It has been proposed that Lnp1/Lunapark stabilizes three-way ER junctions in yeast and mammals (Chen *et al.* 2012, 2015).

We constructed *lem2*Δ cells bearing an extra copy of the *lnp1*$^+$ gene integrated at the *lys1* locus (*lem2*Δ *lnp1*×2). In *lem2*Δ *lnp1*×2 cells, normal growth was rescued. Thus, increased dosage of Lnp1 can compensate the loss of Lem2, although the endogenous level of Lnp1 is not sufficient for the compensation. In addition, cells of the *lem2*Δ *lnp1*Δ double mutant showed severe growth defects in both the rich and the minimum medium (Fig. 6B). These results indicate that Lem2 and Lnp1 have partially redundant roles in regulating cell growth. However, *lem2*Δ cells with an extra copy of the *man1*$^+$ gene integrated at the *lys1* locus (*lem2*Δ *man1*×2) did not compensate the small colony phenotype of *lem2*Δ cells (Fig. 6C). Therefore, it is unlikely that Man1 shares functions with Lem2 in cell growth regulation.

Cells of *lem2*Δ *lnp1*×2 also showed a lower rate of the minichromosome loss (Table 2). In these cells, the level of H3K9me2 at the centromere was rescued to the level observed in wild-type cells in the YES medium (compare '*lem2*Δ *lnp1*×2' with '*lem2*Δ' in Fig. 7B). Interestingly, the level of H3K9me2 at the centromere at *imr* and *dg* repeats was higher in *lem2*$^+$ cells bearing two copies of the *lnp1*$^+$ gene than in wild-type cells (compare '*lnp1*×2'with 'WT' in Fig. 7B). However, levels of H3K9me2 were not significantly different in *lem2*Δ and *lem2*Δ *lnp1*×2 cells in the minimum EMMG medium (Fig. 7B). This finding was consistent with the result that *lem2*Δ phenotypes were most prominent in the rich medium.

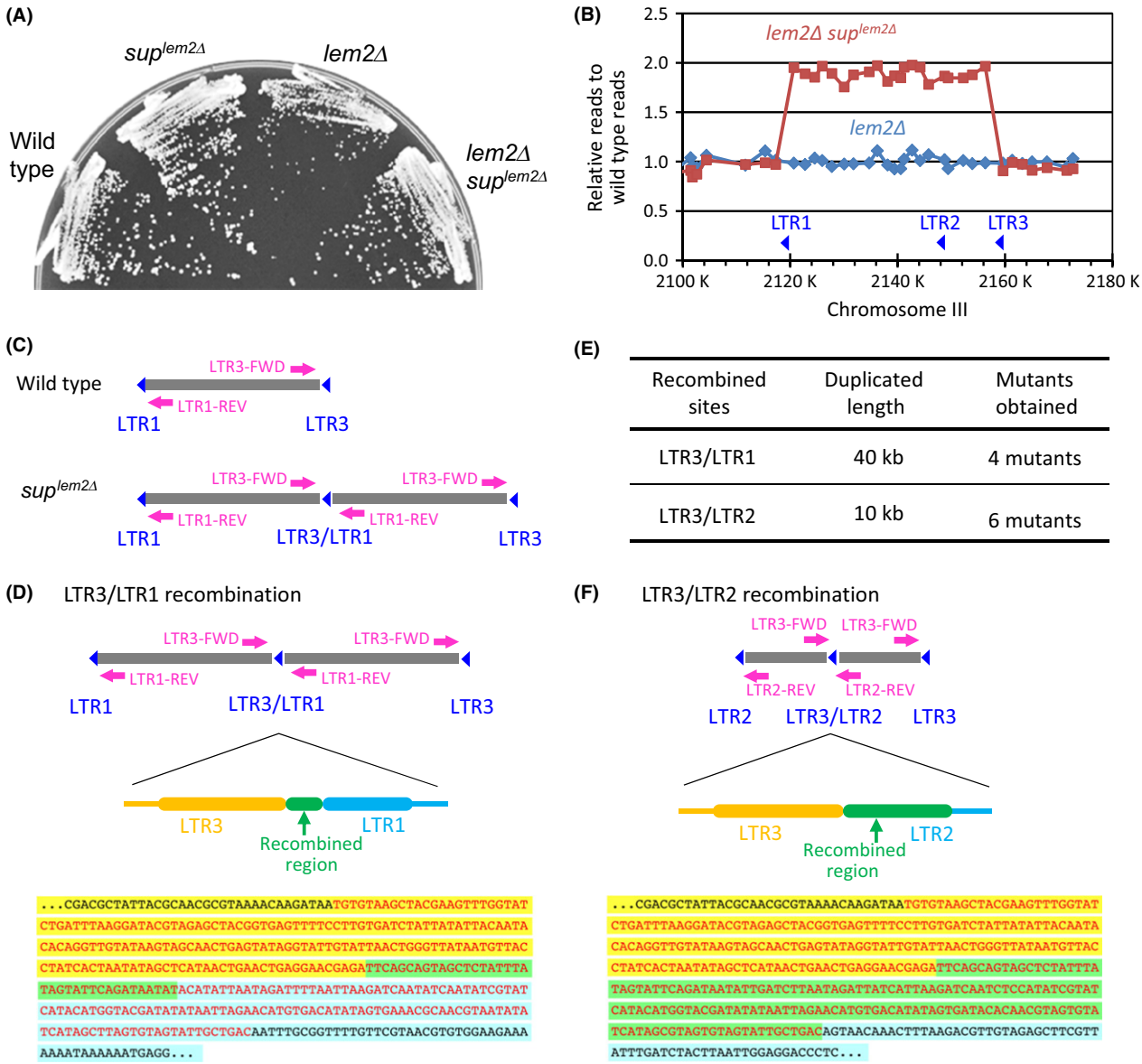

Collectively, these results suggest that Lnp1 augments centromeric heterochromatin formation upon transfer to the rich medium and compensates the loss of Lem2 by restoring centromeric heterochromatin levels.

In an attempt to understand how Lnp1 compensates for the loss of Lem2, we examined the localization of Lnp1 in the presence or absence of Lem2 in the rich YES medium and the minimum EMMG medium. In both culture media, Lnp1-GFP showed dim fluorescence staining at the peripheral regions of the nucleus or ER, indicating a low level of expression. No obvious differences in the localization of Lnp1-GFP were observed in the presence or absence of Lem2 (Fig. 7C). Thus, it is unlikely that Lnp1 can directly substitute for the lost function of Lem2 in the INM when Lem2 is absent (see Discussion).

The MSC domain of Lem2 plays a major role in its functions

To determine functional domains of the Lem2 protein responsible for the observed phenotypes, we

Genes to Cells published by Molecular Biology Society of Japan and John Wiley & Sons Australia, Ltd.

Table 2 Minichromosome loss rate in suppressors of *lem2Δ*

Genotype	Strain name	Minichromosome loss rate (%)
Wild type	YT694	0.017 (12/70601)
lem2Δ	YT2366	10 (87/864)
lem2Δ sup^{lem2Δ}	YT2363	0.18 (96/53337)
Wild type	YT694	<0.01 (5/79994)
lem2Δ	YT2366	9.5 (299/3139)
lnp1×2	YT2442	0.018 (14/78382)
lem2Δ lnp1×2	YT2444	0.038 (19/49899)

Suppression of minichromosome loss of *lem2*Δ by the suppressor mutation. Numbers indicate minichromosome loss rates measured by a half-sector assay in YE: wild-type (YT694), *lem2*Δ (YT2366) and *lem2*Δ *sup^{lem2Δ}* (YT2363) strains.

constructed the following fragments of Lem2 (Fig. 8A): the N-terminal fragment of Lem2 containing the first TM (amino acid residues 1–363; designated Lem2N), Lem2N lacking the first TM (amino acid residues 1–315; designated Lem2N-ΔTM), Lem2N lacking the HEH/LEM domain (Δ11-44; designated Lem2N-ΔLEM) and the C-terminal fragment spanning the first TM of Lem2 (amino acid residues 306–688; designated Lem2C). We integrated these fragments into the chromosome to replace the *lem2$^+$* gene (see Experimental procedures) and examined phenotypes of respective mutant cells. Expression of the Lem2C fragment, which contained the MSC domain, led to a striking reduction in the minichromosome loss in *lem2*Δ cells (Fig. 8B, Table 3). Expression of the Lem2C fragment also rescued the slow growth phenotype of *lem2*Δ cells ('*lem2*Δ + Lem2C' in Fig. 8B). Thus, the Lem2C fragment has a major role in minichromosome stability.

In contrast, the minichromosome loss in *lem2*Δ cells was partially restored by expression of the Lem2N fragment, and this partial rescue was prevented by the lack of either the HEH/LEM domain (Lem2N-ΔLEM) or the first TM (Lem2N-ΔTM) (Fig. 8B, Table 3). Lem2N may exert some effects on chromosomal functions through the HEH/LEM domain when localized to the nuclear envelope.

The combination of mutations in Lem2 and Bqt4 (*lem2*Δ *bqt4*Δ) conferred a synthetic lethal phenotype to *S. pombe* cells (Fig. 9). Bqt4 is an INM protein that is necessary for anchoring telomeres to the nuclear envelope (Chikashige *et al.* 2009). Cells of the *lem2*Δ *bqt4*Δ double mutant terminated growth within several cycles of aberrant cell division after spore germination (Fig. 9A). The synthetic lethal phenotype was rescued again by expression of the Lem2C fragment, but neither by introduction of the Lem2N fragment (Fig. 9B) nor by expression of an extra copy of the *lnp1$^+$* gene (Fig. 9D). These results suggested that the Lem2C fragment is sufficient to compensate the loss of Bqt4 and that the Lem2C fragment and Bqt4 share an essential function of maintaining cell viability. However, none of the truncated Bqt4 fragments examined rescued the synthetic lethal phenotype (Fig. 9C). Even expression of a nearly complete Bqt4 fragment, lacking only the C-terminal TM necessary for nuclear envelope localization, failed to compensate double-mutant phenotypes. This finding showed that Lem2 and Bqt4 perform their essential functions in the nuclear envelope.

Discussion

*Schizosaccharomyces pombe lem2*Δ cells showed phenotypes distinct from those observed in mutations of other known INM proteins. In particular, we noted a high rate of minichromosome loss and defective centromeric heterochromatin formation. The minichromosome loss rate in *lem2*Δ cells was similar to that reported in some mutants defective in the spindle assembly checkpoint (Tange & Niwa 2008). It has been reported that *lem2*Δ cells show an extremely high frequency of the 'cut' (cell untimely torn) phenotype when treated with hydroxyurea (Hayles *et al.* 2013). Furthermore, Rad3-mediated replication checkpoint is severely compromised in *lem2*Δ cells (Xu 2016). These observations suggest that *S. pombe* Lem2 has a regulatory role in checkpoint signaling. However, it has been recently shown that *S. pombe* Lem2 directly affects formation of heterochromatin at centromeres and telomeres (Barrales *et al.* 2016). Roles for Lem2 distinct from those of Man1 in nuclear integrity have also been reported previously (Gonzalez *et al.* 2012). Our present study shows that *S. pombe* Lem2 plays a role in augmentation of heterochromatin formation in response to changes in nutritional conditions.

Two separate pathways involving Lem2 and Lnp1

Although defects in centromeric heterochromatin and slow growth phenotypes were observed in *lem2*Δ cells, these phenotypes were probably separate events, because growth defects have not been reported in well-characterized mutants defective in centromeric heterochromatin formation such as *swi6*Δ or *clr4*Δ. The

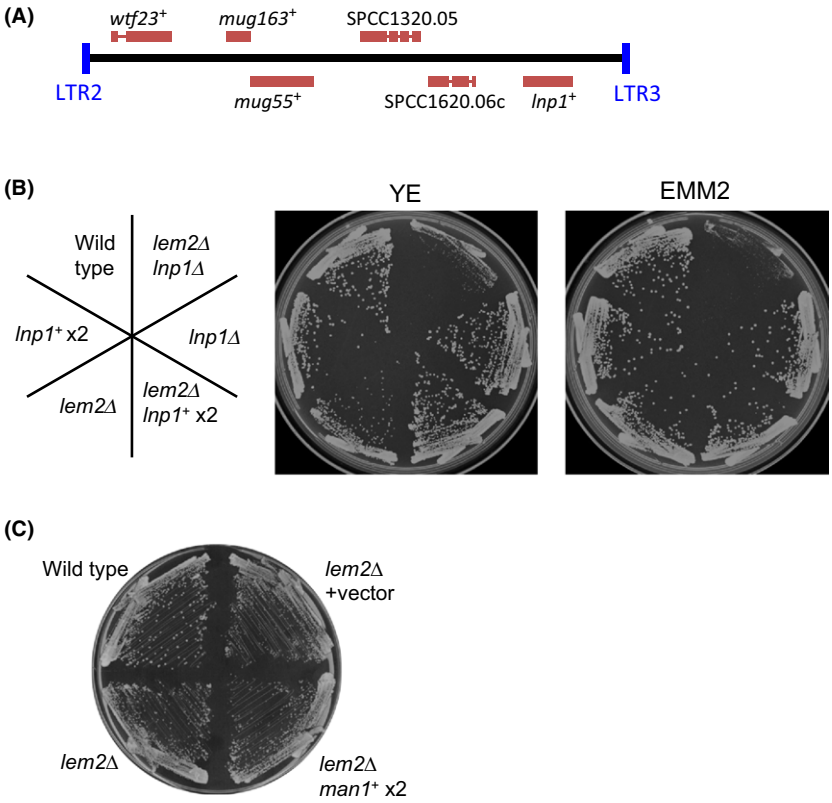

Figure 6 Suppression of effects of Lem2 depletion by Lnp1 duplication. (A) Genes found between LTR2 and LTR3 on chromosome III. Locations of the genes are indicated as brown boxes. (B) Suppression of phenotypes associated with Lem2 depletion by Lnp1 duplication. Strains of indicated genotypes on the left were inoculated on the YE or EMM2 plate medium and incubated at 30 °C for 2 (YE) or 3 days (EMMG). Then, colony sizes were compared. The following strains were used: wild type, YT2414; *lem2*Δ *lnp1*Δ, YT2425; *lem2*Δ *lnp1*$^+$×2, YT2417; *lem2*Δ, YT2416; and *lnp1*$^+$×2, YT2415. (C) Man1 does not rescue the slow growth phenotype of *lem2*Δ cells. Strains of indicated genotypes were inoculated on the YE plate medium and incubated at 30 °C for 2 days. The following strains were used: wild type, YT2414; *lem2*Δ, YT2416; *lem2*Δ+vector, YT2555; and *lem2*Δ+*man1*$^+$x2, YT2554. LTR, long-terminal repeat.

slow growth phenotype in *lem2*Δ cells may reflect reduced viability in vegetative culture as previously detected by the staining of dead cells with phloxine B (Gonzalez *et al.* 2012). Interestingly, these phenotypes in *lem2*Δ cells were suppressed by a duplication of the *lnp1*$^+$ gene (Figs 6B and 7B). Similarly, defective centromeric heterochromatin in *lem2*Δ cells was also suppressed by an increased expression of Lnp1 (Barrales *et al.* 2016). A possible explanation for this compensation is that up-regulated Lnp1 may extend its localization beyond the ER membrane to the nuclear membranes in the absence of Lem2 and functionally substitute for the latter protein. However, the detected protein levels of Lnp1 were much lower than those of Lem2, and no obvious changes in the localization of Lnp1 occurred in the absence or presence of Lem2 (Fig. 7C). Therefore, it is unlikely that Lnp1 directly substitutes for the function of Lem2. In addition, Lnp1 duplication leads to an increased accumulation of H3K9me2 at the centromeric heterochromatin in the rich YES medium regardless of the presence or absence of Lem2 (Fig. 7B). Thus, we wish to emphasize the possibility that Lnp1-dependent suppression may be caused, at least in part, through as yet unknown metabolic pathways that are also engaged in nutrition signaling. Here, we suggest the presence of separate Lem2-mediated and Lnp1-mediated pathways for the augmentation of heterochromatin as illustrated in Fig. 10. The nutrition-dependent accumulation of Lem2 at CENP-A chromatin mediates H3K9me2 accumulation at the outer regions of the centromere. H3K9me2 accumulation also occurs downstream of Lnp1 independently of Lem2. In contrast, the synthetic lethal phenotype of the *lem2*Δ *bqt4*Δ double mutant does not depend on the nutrition status and is not rescued by a duplication of the *lnp1*$^+$ gene (Fig. 9D). Thus,

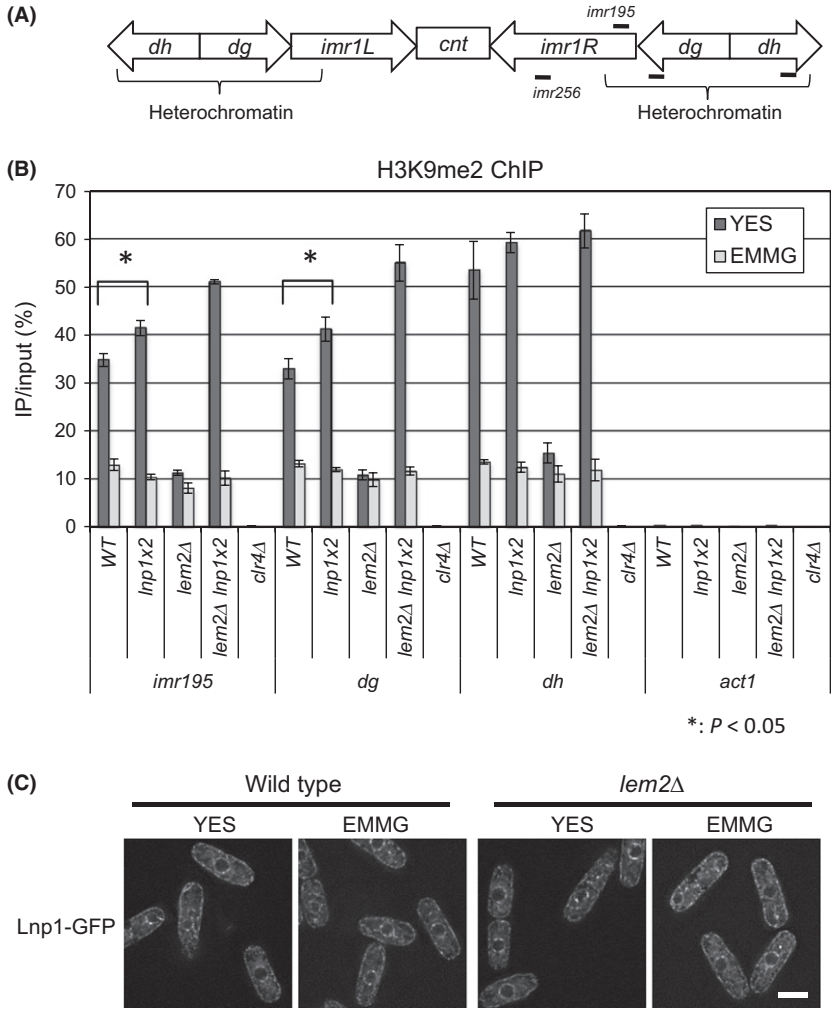

Figure 7 Centromeric heterochromatin in *lem2*Δ suppressors. (A) Schematic representation of centromere 1. Black bars indicate the positions of the PCR products in the chromatin immunoprecipitation (ChIP) assay (imr, dg and dh). (B) ChIP analysis of H3K9me2 at the indicated loci in the indicated strains grown in YES or EMMG. Relative ratios of immunoprecipitated DNA to input DNA are indicated. Statistical significance was determined using the two-sided Student's *t*-test. (C) Subcellular localization of Lnp1-GFP in living cells. Wild-type and *lem2*Δ cells (YT2453 and YT2454) grown in YES or EMMG medium were observed by fluorescence microscopy. Scale bar, 5 μm.

overlapping functions of Lem2 and Bqt4 essential for cell viability are independent of the Lnp1-mediated pathway.

Functional domains of Lem2

In *S. pombe*, it has been recently shown that the N-terminal HEH/LEM domain and the C-terminal MSC domain of Lem2 have distinct functions. The HEH/LEM domain mediates association with chromatin and tethering of centromeres to the nuclear envelope, whereas the MSC domain mediates silencing of centromeric heterochromatin (Barrales *et al.* 2016). The *S. pombe* HEH/LEM domain in both Lem2 and Man1 anchors chromatin to the nuclear envelope (Gonzalez *et al.* 2012). The metazoan LEM domain binds to the barrier-to-autointegration factor (BAF) (Haraguchi *et al.* 2001; Lee *et al.* 2001; Shumaker *et al.* 2001). BAF is a DNA binding protein that was initially discovered as the host cell protein that facilitated integration of HIV viral DNA into the host genome by preventing the viral DNA from suicidal autointegration (Chen & Engelman 1998; Lee & Craigie 1998). Because *S. pombe* has no

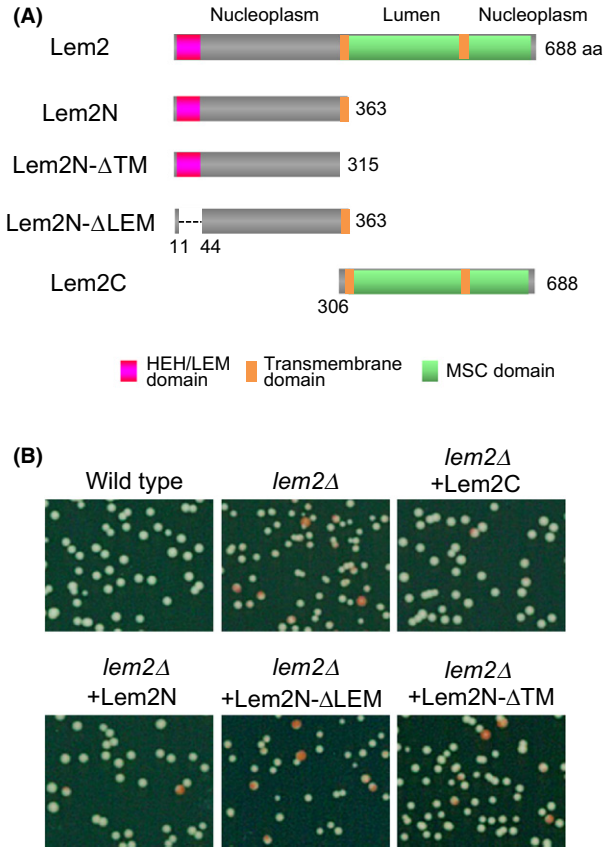

Figure 8 Functional domains of Lem2. (A) Schematic of the *S. pombe* Lem2 protein and Lem2 fragments. The helix-extension-helix (HEH)/LEM domain and two transmembrane (TM) domains are labeled. Broken line indicates the deleted region of HEH/LEM domain in Lem2N-ΔLEM. (B) Suppression of the *lem2*Δ phenotype by Lem2 fragments. The minichromosome loss assay was carried out in *lem2*Δ strains harboring the full-length *lem2* fragment (YT2529), Lem2N (YT2531), Lem2N-ΔTM (YT2530), Lem2N-ΔLEM (YT2532) and Lem2C (YT2533). Colonies grown on a YE plate are shown. *lem2*Δ (YT2535) strain was also studied as a control.

homologues of BAF, the *S. pombe* HEH/LEM domain may bridge chromatin to the nuclear envelope directly or through yet unknown proteins. However, tethering of telomeres to the nuclear envelope and silencing of telomeric heterochromatin are both mediated by the MSC domain of Lem2 (Barrales *et al.* 2016). Our study showed that expression of the MSC domain of *S. pombe* Lem2 compensated the phenotypes of the minichromosome loss and slow growth in *lem2*Δ cells. Expression of this domain also compensated the synthetic lethal phenotype of *lem2*Δ *bqt4*Δ cells. Thus, the C-terminal MSC domain of Lem2 has a major regulatory influence on chromatin.

Table 3 Minichromosome loss rates in *lem2Δ* cells expressing Lem2 fragments

Genotypes/Fragment	Strain names	Minichromosome loss rate (%)
lem2Δ	YT2535	9.0 (171/1894)
lem2Δ/Lem2C	YT2533	0.16 (3/1885)
lem2Δ/Lem2N	YT2531	1.9 (69/3651)
lem2Δ/Lem2N-ΔLEM	YT2532	13.7 (224/1636)
lem2Δ/Lem2N-ΔTM	YT2530	7.4 (136/1836)

Suppression of minichromosome loss in *lem2*Δ by Lem2 fragments. Numbers indicate minichromosome loss rates measured by a half-sector assay in YE.

Despite the similarity of domain structures in Lem2 and Man1, these two proteins apparently have distinct roles in cell growth regulation as the phenotypes of slow growth and minichromosome loss in *lem2*Δ were not compensated by expression of an extra copy of *man1* (Fig. 6C) and because *man1*Δ, unlike *lem2*Δ, had no genetic interaction with *bqt4*Δ (Fig. 9D). Therefore, regulation of cell growth by Lem2 is specifically mediated by its MSC domain.

Importance of Lem2 for centromere function

We showed that Lem2 binds to CENP-A chromatin of the centromere and thereby enhances heterochromatin formation at the outer centromeric regions in parallel with the RNAi-dependent pathway. This result is consistent with a recent report by Barrales *et al.* (2016) and suggests that one role of Lem2 is to anchor CENP-A chromatin to the nuclear envelope, providing a platform for the enhancement of heterochromatin formation at the outer centromeric regions. It is expected that the presence of the minichromosome may consume more proteins required for heterochromatin formation, thus causing more severe growth defects. This notion may explain why the *lem2*Δ cells that had lost the minichromosome grew faster than those bearing it did.

A striking new finding of the present study was that Lem2-mediated centromeric heterochromatin formation depended on the nutritional status: centromeric heterochromatin formation was augmented when wild-type cells were moved to the rich medium; however, this augmentation did not occur in the absence of Lem2 (Fig. 4A). Thus, it is possible that Lem2 regulates heterochromatin formation by acting downstream of nutritional signaling. This idea is supported by the fact that epigenetic modification patterns of chromatin are altered by cellular

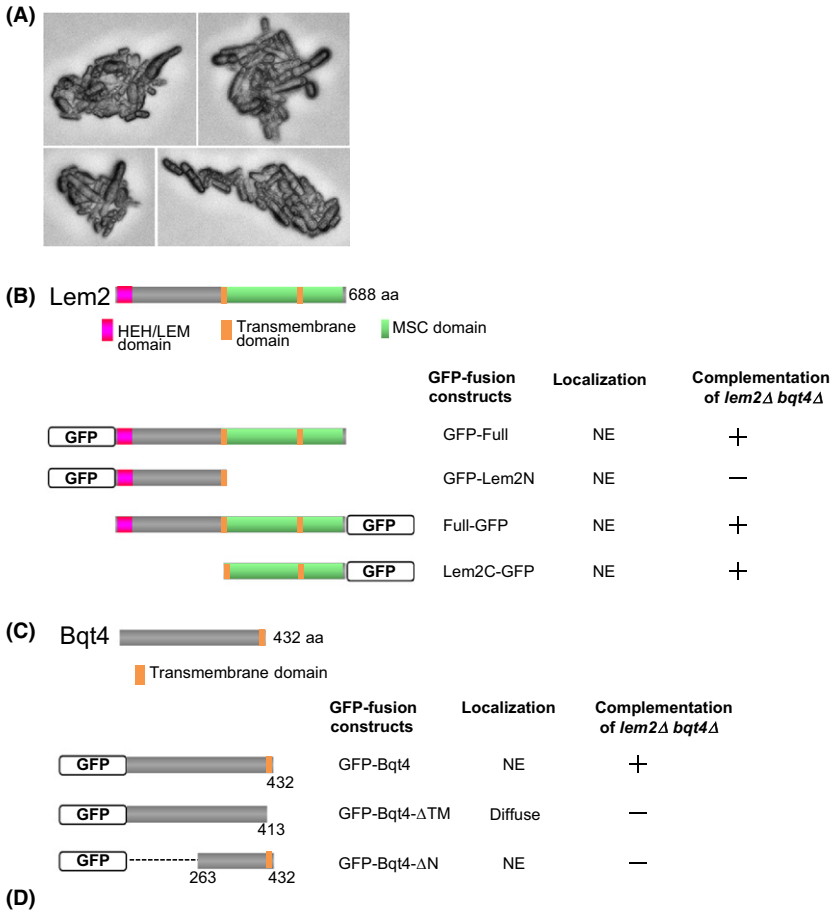

(D)

Genotype	Growth
*lem2*Δ *bqt4*Δ	Lethal
*lem2*Δ *bqt4*Δ *lnp1* x2	Lethal
*man1*Δ *bqt4*Δ	Viable
*lem2*Δ *rap1*Δ	Viable

Figure 9 Synthetic lethality of the combined *lem2*Δ *bqt4*Δ mutation. (A) Terminal phenotype of *lem2*Δ *bqt4*Δ cells. Spores were germinated after tetrad dissection and observed under a bright-field microscope. (B, C) Complementation of *lem2*Δ *bqt4*Δ by Lem2 or Bqt4 fragments. '+'indicates that the fragment complemented the lethal phenotype of the *lem2*Δ *bqt4*Δ double mutant; '–' indicates a failure to complement the lethal phenotype. Localization of each fragment in interphase cells is also indicated. For localization: NE, nuclear envelope. (D) Genetic interactions among nuclear membrane proteins and telomere proteins.

metabolism (reviewed in Meier 2013; Keating & El-Osta 2015). It has been also suggested that the LEM-domain proteins in metazoans regulate TGFβ signaling during differentiation (reviewed in Bengtsson 2007). These findings provide general insight into a role for the nuclear envelope acting as a platform for transduction of extracellular and intracellular signals to chromatin.

Although it was previously reported that Csi1 is required to connect centromeres to the SPB (Hou *et al.* 2012), Lem2 and Csi1 were proposed to have additive roles in mediating the centromere–SPB connection (Barrales *et al.* 2016). Our study complements those findings by showing additive effects of *lem2*Δ and *csi1*Δ mutations on the minichromosome loss. Therefore, the Lem2-mediated potentiation of centromeric heterochromatin formation additively contributes to the Csi1-mediated centromere–SPB connection and, thereby, to minichromosome stability. It also merits a comment that *csi1*Δ cells grew

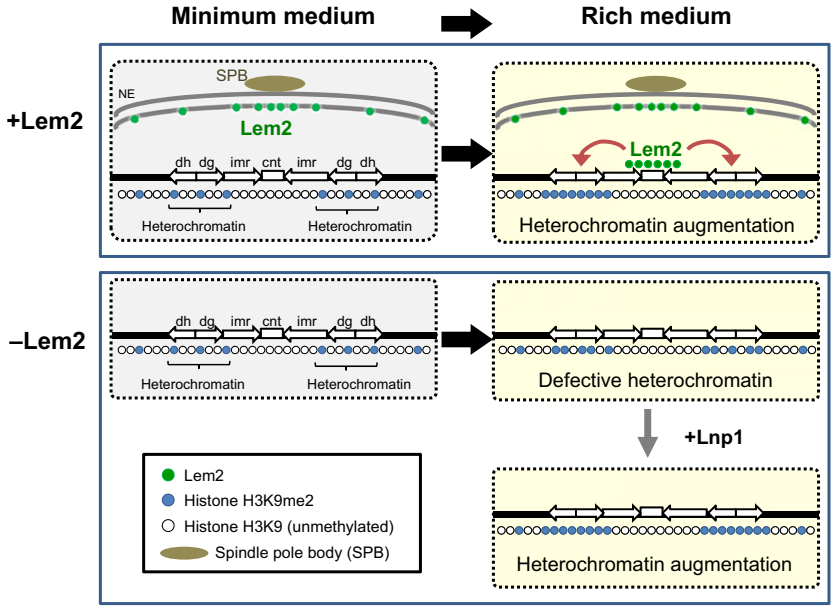

Figure 10 Lem2-mediated, nutrition-dependent formation of centromeric heterochromatin. (Upper panel indicated by '+Lem2') Upon transfer to a nutritionally rich condition, Lem2 associates with CENP-A chromatin at the inner centromere region and augments heterochromatin formation at the outer centromeric regions in wild-type cells. (Lower panel indicated by '-Lem2') In the absence of Lem2, the centromeric heterochromatin formation is insufficient. This phenotype is rescued by the additional expression of Lnp1. Green circles, Lem2; blue circles, chromatin containing methylated histone H3K9; and white circles, chromatin containing unmethylated histone H3K9.

similarly well in the presence or absence of the minichromosome, unlike *lem2*Δ cells. Another notable difference between these mutants is that the *csi1*Δ phenotypes were observed in both the rich medium and the minimum medium, whereas the *lem2*Δ phenotypes were only prominent in the rich medium. These results suggest that Lem2 and Csi1 play distinct roles and regulate minichromosome stability through separate mechanisms.

Importance of Lem2 for telomere function

Our study showed a synthetic interaction of Lem2 with the Bqt4 telomere protein that affected cell viability. It is possible that the loss of viability in the *lem2*Δ *bqt4*Δ double mutant is caused by telomere defects as the MSC domain of Lem2 mediates telomere anchoring and heterochromatin silencing (Barrales *et al.* 2016). However, it is unlikely that Bqt4 directly influences heterochromatin formation because telomeres are detached from the nuclear envelope in the absence of Bqt4 whereas telomere silencing is still maintained (Chikashige *et al.* 2009, 2010). Moreover, *lem2*Δ did not show a synthetic lethal phenotype when combined with *rap1*Δ (Fig. 9D). Rap1 is a telomere protein that anchors telomeres to the nuclear envelope through the interaction with Bqt4 (Chikashige et al. 2009; Chikashige & Hiraoka 2001). Thus, the synthetic lethal phenotype of *lem2*Δ *bqt4*Δ cells may not be due to dysregulation of telomere functions of Bqt4. Nontelomeric functions of Bqt4 have not been shown yet; thus, our findings will stimulate new studies of interactions of Bqt4 with Lem2.

Regulation of LTR stability by Lem2

Although defective centromeric heterochromatin formation is obviously manifested as a failure of chromosome segregation, it is tempting to speculate that defective heterochromatin is not limited to centromeres or telomeres, but also occurs at other heterochromatic regions in the genome. Spontaneous duplication of genomic sequences that generated suppressors of *lem2*Δ cells implied the occurrence of recombination at the LTR sequences due to their derepression. In *S. pombe*, it has been reported that CENP-B homologues (Cbp1/Abp1, Cbh1 and Cbh2) repress transcriptional and recombinational activities of LTR sequences by recruiting histone deacetylases (Cam *et al.* 2008). Furthermore, CENP-B homologues

promoted progression of replication forks through the LTR (Zaratiegui *et al.* 2011). As CENP-B was localized to centromeres as well as to LTR sequences, it is possible that Lem2 may affect these chromosomal regions together with CENP-B. This also suggests that Lem2 can act on other chromosomal regions located closely to the nuclear envelope. In summary, we propose that Lem2 provides a platform for chromatin and, thereby, maintains genome stability, which is one of the principal functions of the nuclear envelope.

Experimental procedures

Strains and culture media

Schizosaccharomyces pombe strains used in this study are listed in Table S1 (Supporting information). Culture media for *S. pombe* are described in Moreno *et al.* (1991). YES was used as a rich medium in most experiments. For the minichromosome loss assay, YE was used as a rich medium. EMM supplemented with 5 g/L glutamate (substituted for NH_4Cl) as a nitrogen source (EMMG) was used as a minimum medium.

Constructs

Gene disruption and gene replacement were carried out by the direct chromosomal integration method (Wach 1996; Bähler *et al.* 1998). The pFA6-KanMX6, pCR2.1-hph and pCR2.1-nat plasmids were used to generate integration cassettes (Bähler *et al.* 1998; Sato *et al.* 2005). To replace the chromosomal *lem2*$^+$ gene with a truncated fragment, strains in which the chromosomal *lem2*$^+$ gene was deleted with the *ura4*$^+$ cassette were transformed with truncated gene fragments. Transformants were screened on plates with the EMMG medium that contained 5-fluoroorotic acid to eliminate clones harboring *ura4*$^+$. Correct replacements were confirmed by genomic PCR.

To express the *lnp1*$^+$ gene, a genomic DNA region containing the entire ORF (SPCC1620.07c; −709 to +2560 from the beginning of the protein coding sequence) was amplified by PCR. To express the *man1*$^+$ gene, a genomic DNA region containing entire ORF (−326 to +3338 from the beginning of the protein coding sequence) was amplified by PCR. Amplified DNA molecules were cloned into the pYC36 plasmid (Chikashige *et al.* 2004) that harbored the *lys1* marker. For Fig. 7C, the GFP gene was fused to the 3′ end of the *lnp1*$^+$ ORF. Every gene located within the 40-kb duplicated region of the chromosome III was also cloned with its promoter region into the pYC36 plasmid. To express the *lem2*$^+$ gene fragment from the *lys1* locus, gene fragments were amplified by PCR and cloned under the *lem2* promoter into the pYC36 plasmid. Plasmids harboring GFP-*bqt4* fusion genes were described previously (Chikashige *et al.* 2009). The plasmids were integrated into the genomic *lys1-131* locus of host strains. Correct integration was confirmed by genomic PCR.

Immuno-electron microscopy

Cells expressing Lem2-GFP or GFP-Lem2 were cultured in the YES medium, After washing with 0.1 M phosphate buffer (PB, pH7.4), cells (1×10^8 cells/mL) were fixed with a fixative (4% formaldehyde and 0.01% glutaraldehyde dissolved in PB) for 20 min at room temperature and washed with PB three times for 5 min each. Then, cells were treated with 0.5 mg/mL Zymolyase 100T (Seikagaku Co.) in PB for 20 min at 30 °C and washed with PB three times. After two successive treatments with 100 mM lysine HCl in PB for 10 min each and subsequent washing with PB, cells were permeabilized for 15 min with PB containing 0.2% saponin and 1% bovine serum albumin (BSA) and incubated at 4 °C overnight with a primary antibody (rabbit polyclonal anti-GFP antibody, Rockland) diluted at 1 : 400 in PB containing 1% BSA and 0.001% saponin. After three 10-min washes with PB containing 0.005% saponin, cells were incubated for 2 h at room temperature with a secondary antibody (goat anti-rabbit Alexa 594 FluoroNanogold Fab' fragment; Nanoprobes, Inc.) diluted at 1 : 100 in PB containing 1% BSA and 0.001% saponin. Then, cells underwent three 10-min washes with PB containing 0.005% saponin and one final wash with pure PB. Then, the cells were fixed again with 1% glutaraldehyde in PB for 1 h, washed with PB once and treated with 100 mM lysine HCl in PB twice for 10 min each. The cells were stored at 4 °C until use. Before use, the cells were incubated with 50 mM HEPES (pH 5.8) three times for 3 min each, incubated with the silver enhancement reagent (a mixture of equal volumes of the following A, B and C solutions: A - 0.2% silver acetate solution; B - 2.8% trisodium citrate-$2H_2O$, 3% citric acid-H_2O and 0.5% hydroquinone; C - 200 mM HEPES, pH 6.8) at 25 °C for 7 min and washed three times with distilled water (DW). Cells were embedded in 2% low-melting agarose dissolved in DW. Then, cells were post-fixed with 2% OsO_4 in DW for 15 min at room temperature, washed three times with DW, stained with 1% uranyl acetate in DW for 1 h and then again washed three times with DW.

Cells were dehydrated with ethanol using sequential incubations with 50% and 100% ethanol for 10 min each and finally with acetone for 10 min. For embedding in epoxy resin, cells were incubated sequentially with mixtures of acetone–Epon812 (1 : 1) for 1 h, acetone–Epon812 (1 : 2) for 1 h, in Epon812 overnight and in Epon812 again for another 3 h. Then, the preparation was left to stand until it solidified. The blocks containing cells were sectioned with a microtome instrument (Leica Microsystems), and the ultrathin sections were doubly stained with 4% uranyl acetate for 20 min and lead citrate (Sigma) for 1 min as a usual pre-treatment for EM observations.

Minichromosome loss assay

Minichromosome loss assay was carried out as described (Allshire *et al.* 1995). Briefly, cells harboring minichromosome Ch16 (Matsumoto *et al.* 1987) were precultured in the

EMMG liquid medium supplemented with 50 μg/mL leucine, then plated on YE plates and incubated at 30 °C for 3–4 days. For quantification, the number of colonies which had at least half of the colony turned red was counted. The rate of the minichromosome loss was calculated by dividing the number of half-sectored colonies by the total number of white and half-sectored colonies. It should be noted that the rate of the minichromosome loss can be accurately calculated by the half-colony assay only when the minichromosome loss is a rare event. When the rate is high enough and frequent minichromosome loss occurs in cells during colony formation, this assay may lead to overestimation of the rate value (Allshire *et al.* 1995).

Whole-genome sequencing

The *lem2*Δ *sup*$^{lem2\Delta}$ (YT2327) strain was crossed with a wild-type strain (972), and the four generated tetrads were separated and checked for their colony size. The *lem2*$^{+}$ progenies were further crossed with *lem2*Δ to obtain the *lem2*Δ background and checked for colony size to confirm whether they comprised *sup*$^{lem2\Delta}$. A tetratype tetrad (strains YT2565, YT2566, YT2567 and YT2568) was selected for whole-genome sequencing. Genomic DNA was isolated from an isogenic set of wild-type, *lem2*Δ, *lem2*Δ *sup*$^{lem2\Delta}$ and *sup*$^{lem2\Delta}$ cells using a Qiagen Blood & Cell Culture DNA Kit (Cat. no. 13323). Whole-genome sequencing using Illumina Genome Analyzer and data mining was carried out by Takara Bio Inc.

PCR and sequencing of LTR recombination loci

Genomic DNA was purified from *S. pombe* cells using a Qiagen Blood & Cell Culture DNA Kit (Cat. no. 13323). DNA fragments were amplified using genomic DNA as a template and the following set of primers: LTR1-REV (5′-CAATTT TATATCAAAAATCTAGTCC-3′), LTR2-REV (5′-ATGG GATCAATGTTTACCGTGAA-3′) and LTR3-FWD (5′-GCCAGTGTAAATAGATGATGATTC-3′). PCR products are expected to be generated only when duplication occurs between the LTRs. Nucleotide sequences of PCR products were determined by an Applied Biosystems 3130XL Genetic Analyzer.

ChIP assay

Chromatin immunoprecipitation experiments were conducted as previously described (Kawakami *et al.* 2012).

Cells (2.5×10^8) were fixed with 1% formaldehyde (Nacalai Tesque) in the YES medium for 20 min at 25 °C. After quenching fixation with 150 mM glycine, cells were harvested and washed twice with Buffer 1 (50 mM HEPES, 140 mM NaCl, 1 mM ethylenediaminetetraacetic acid (EDTA), 1% Triton X-100 and 0.1% Na-deoxycholate, pH 7.5). The cell pellet was resuspended in Buffer 1 containing a protease inhibitor cocktail diluted at 1 : 20 (Nacalai Tesque) and homogenized with a bead shocker (Yasui Kikai, Co.). The cell extract was made up to 2 mL with Buffer 1 containing protease inhibitor cocktail (1 : 100) and sonicated for 240 s with Biorupter UCW-310 (Cosmo Bio, Co.) set at level 'H'. After sonication, the cell extract was centrifuged at 15 000 rpm for 15 min. The input fraction was used for immunoprecipitation with secondary antibody-conjugated magnetic beads (Dynal). Anti-myc (4A6/Millipore), anti-H3K9me2 (a gift from T. Urano, Shimane University), anti-Cnp1 (Takayama *et al.* 2008) and anti-histone H3 (Millipore) antibodies were used. Magnetic beads (50 μL) were pre-incubated with 1.5 μg of the antibody for 1 h at 4 °C before incubation with cell extracts. After immunoprecipitation, the beads were washed with Buffer 1 and then twice with each of the following three buffers: Buffer 1' (50 mM HEPES, 500 mM NaCl, 1 mM EDTA, 1% Triton X-100 and 0.1% Na-deoxycholate, pH 7.5), Buffer 2 (10 mM Tris, 250 mM LiCl, 0.5% NP-40 and 0.5% Na-deoxycholate, pH 8.0) and TE buffer (10 mM Tris, 1 mM EDTA, pH 8.0). Beads were resuspended and incubated for 10 min at 37 °C in the TE buffer containing 100 μg/mL RNase A. Then, proteinase K (0.5 mg/mL) was added and the mixture was digested for another 2 h at 37 °C. After de-cross-linking, DNA was purified using a QIAquick PCR purification kit (Qiagen). qPCR was carried out using SYBR premix Ex-Taq (Takara Bio, Inc.) and the Thermal Cycler Dice Real Time system TP800 (Takara Bio, Inc.). The primers used for gene-specific cDNA synthesis and for qPCR are listed in Table S2 (Supporting information). For the time-course experiment, cells were grown in 500 mL of the EMMG media until the concentration of 1.0×10^7 cells/mL and harvested by centrifugation. Harvested cells were washed once with phosphate-buffered saline (PBS) and then inoculated in 500 mL of the YES media. After the media shift, cells were cross-linked with 1% formaldehyde for ChIP assay at 0, 2, 4, 6, 8 and 12 h. Experiments were carried out in triplicate to achieve biological reproducibility.

Western blot analysis

Western blotting was carried out as described previously (Asakawa *et al.* 2014) with slight modifications. *S. pombe* cells expressing Lem2-GFP (cYK183-3A) were cultured in the YES or EMMG medium to log phase for 24 h. After NaOH/trichloroacetic acid precipitation, the pellets were resuspended in sample buffer and subjected to sodium dodecyl sulfate polyacrylamide gel electrophoresis (SDS-PAGE) on a 10% polyacrylamide gel. After SDS-PAGE, the proteins were transferred to a polyvinylidene fluoride (PVDF) membrane by wet transfer. The membrane was blocked in 5% skim milk and incubated with a rabbit polyclonal anti-GFP antibody (2.5 μg/mL; Rockland Immunochemicals Inc.) for overnight at 4 °C. The membrane was washed with PBS containing 0.05% Tween®-20 three times and then incubated with horseradish peroxidase (HRP)-conjugated donkey anti-rabbit IgG (1 : 5000; GE Healthcare) for 2 h at room temperature. Bands were detected by chemiluminescence using a ChemiDoc™

MP imaging system (Bio-Rad). For the loading control, actin was detected by a mouse monoclonal anti-β-actin antibody (1.5 μg/mL; Abcam) and an HRP-conjugated sheep anti-mouse IgG.

Genetic interactions

Synthetic lethality of the *lem2*Δ *bqt4*Δ double mutant was assayed by the tetrad analysis of the following cross, HMP1592R (*h*$^+$ *his2-245 leu1-32 ura4-D18 ade6-210 lem2*Δ*::ura4*$^+$) × CRLx08 (*h*$^-$ *leu1-32 lys1-131 ura4-D18 ade6-216 bqt4*Δ*::hph*). The viable *lem2*Δ *bqt4*Δ double mutant was not found in segregants of more than 28 tetrads. Germination of spores that were assumed to have the genotype of *lem2*Δ *bqt4*Δ double mutant was checked microscopically on the agar plate after dissection of tetrad spores. Similarly, to determine the synthetic effect of *lem2*Δ *bqt4*Δ *lnp1*×2, *man1*Δ *bqt4*Δ or *lem2*Δ *rap1*Δ, tetrad analysis was carried out for the following crosses, respectively: CRLo13e × CRLo14v, CRLt84× YT2233 or CRLy14× CRLo164.

Complementation of the *lem2*Δ *bqt4*Δ double mutant by the Lem2 partial fragments was examined using the tetrad analysis of the following cross: CRLo13e crossed with the *bqt4*Δ strain bearing a truncated *lem2*$^+$ gene at the *lys1* locus (CRLo14s, CRLo16 m, CRLo14t or CRLo158; genotypes indicated in Table S1 in Supporting Information listed for Fig. 9B). Complementation of the *lem2*Δ *bqt4*Δ double mutant by the Bqt4 partial fragments was examined by the tetrad analysis of the following cross, CRLo163× CRLs03, or CRLu50.

Microscopic observation

YT2453 (*lnp1*$^+$*-GFP*) and YT2454 (*lem2Δ lnp1*$^+$*-GFP*) were cultured in YES or EMMG medium overnight at 30 °C to the logarithmic growth phase. Intracellular localization of GFP fusion proteins was observed in living *S. pombe* cells by a DeltaVision™ fluorescence microscope system (Applied Precision, Inc.) equipped with a CoolSNAP™ HQ2 CCD (Photometrics) using an Olympus oil-immersion objective lens (PlanApoN60 OSC, NA = 1.4). After deconvolution, five z-stack images each corresponding to an optical slice of 0.2 μm thickness were projected. The brightness of the images was changed for better presentation using Fiji software (Schindelin *et al.* 2012) without changing the gamma.

Acknowledgements

We thank Chizuru Ohtsuki and Yasuha Kinugasa for technical support, Atsuhi Matsuda for providing the *man1*Δ *bqt4*Δ double-mutant *S. pombe* strain and Takeshi Urano for providing anti-H3K9me2 antibody. This work was supported by JSPS KAKENHI to H.A. (grant number 26440098), Y.M. (25250022), T.H. (25116006) and Y.H. (26116511 and 26251037).

References

Allshire, R.C., Nimmo, E.R., Ekwall, K., Javerzat, J.P. & Cranston, G. (1995) Mutations derepressing silent centromeric domains in fission yeast disrupt chromosome segregation. *Genes Dev.* **9**, 218–233.

Alper, B.J., Lowe, B.R. & Partridge, J.F. (2012) Centromeric heterochromatin assembly in fission yeast – balancing transcription, RNA interference and chromatin modification. *Chromosome Res.* **20**, 521–534.

Asakawa, H., Yang, H.J., Yamamoto, T.G., Ohtsuki, C., Chikashige, Y., Sakata-Sogawa, K., Tokunaga, M., Iwamoto, M., Hiraoka, Y. & Haraguchi, T. (2014) Characterization of nuclear pore complex components in fission yeast *Schizosaccharomyces pombe*. *Nucleus* **5**, 149–162.

Bähler, J., Wu, J.Q., Longtine, M.S., Shah, N.G., McKenzie, A., Steever, A.B., Wach, A., Philippsen, P. & Pringle, J.R. (1998) Heterologous modules for efficient and versatile PCR-based gene targeting in *Schizosaccharomyces pombe*. *Yeast* **14**, 943–951.

Barrales, R.R., Forn, M., Georgescu, P.R., Sarkadi, Z. & Braun, S. (2016) Control of heterochromatin localization and silencing by the nuclear membrane protein Lem2. *Genes Dev.* **30**, 133–148.

Barton, L.J., Soshnev, A.A. & Geyer, P.K. (2015) Networking in the nucleus: a spotlight on LEM-domain proteins. *Curr. Opin. Cell Biol.* **34**, 1–8.

Bengtsson, L. (2007) What MAN1 does to the Smads. TGFβ/BMP signaling and the nuclear envelope. *FEBS J.* **274**, 1374–1382.

Berk, J.M., Tifft, K.E. & Wilson, K.L. (2013) The nuclear envelope LEM-domain protein emerin. *Nucleus* **4**, 298–314.

Bione, S., Maestrini, E., Rivella, S., Mancini, M., Regis, S., Romeo, G. & Toniolo, D. (1994) Identification of a novel X-linked gene responsible for Emery-Dreifuss muscular dystrophy. *Nat. Genet.* **8**, 323–327.

Brachner, A. & Foisner, R. (2011) Evolvement of LEM proteins as chromatin tethers at the nuclear periphery. *Biochem. Soc. Trans.* **39**, 1735–1741.

Brachner, A., Reipert, S., Foisner, R. & Gotzmann, J. (2005) LEM2 is a novel MAN1-related inner nuclear membrane protein associated with A-type lamins. *J. Cell Sci.* **118**, 5797–5810.

Buch, C., Lindberg, R., Figueroa, R., Gudise, S., Onischenko, E. & Hallberg, E. (2009) An integral protein of the inner nuclear membrane localizes to the mitotic spindle in mammalian cells. *J. Cell Sci.* **122**, 2100–2107.

Buscaino, A., Lejeune, E., Audergon, P., Hamilton, G., Pidoux, A. & Allshire, R.C. (2013) Distinct roles for Sir2 and RNAi in centromeric heterochromatin nucleation, spreading and maintenance. *EMBO J.* **32**, 1250–1264.

Cam, H.P., Noma, K., Ebina, H., Levin, H.L. & Grewal, S.I. (2008) Host genome surveillance for retrotransposons by transposon-derived proteins. *Nature* **451**, 431–436.

Chen, H. & Engelman, A. (1998) The barrier-to-autointegration protein is a host factor for HIV type 1 integration. *Proc. Natl Acad. Sci. USA* **95**, 15270–15274.

Chen, S., Desai, T., McNew, J.A., Gerard, P., Novick, P.J. & Ferro-Novick, S. (2015) Lunapark stabilizes nascent three-way junctions in the endoplasmic reticulum. *Proc. Natl Acad. Sci. USA* **112**, 418–423.

Chen, S., Novick, P.J. & Ferro-Novick, S. (2012) ER network formation requires a balance of the dynamin-like GTPase Sey1p and the Lunapark family member Lnp1p. *Nat. Cell Biol.* **14**, 707–716.

Chikashige, Y., Ding, D.Q., Funabiki, H., Haraguchi, T., Mashiko, S., Yanagida, M. & Hiraoka, Y. (1994) Telomere-led premeiotic chromosome movement in fission yeast *Schizosaccharomyces pombe*. *Science* **264**, 270–273.

Chikashige, Y., Haraguchi, T. & Hiraoka, Y. (2007) Another way to move chromosomes. *Chromosoma* **116**, 497–505.

Chikashige, Y., Haraguchi, T. & Hiraoka, Y. (2010) Nuclear envelope attachment is not necessary for telomere function in fission yeast. *Nucleus* **1**, 481–486.

Chikashige, Y. & Hiraoka, Y. (2001) Telomere binding of the Rap1 protein is required for meiosis in fission yeast. *Curr. Biol.* **11**, 1618–1623.

Chikashige, Y., Kurokawa, R., Haraguchi, T. & Hiraoka, Y. (2004) Meiosis induced by inactivation of Pat1 kinase proceeds with aberrant nuclear positioning of centromeres in the fission yeast *Schizosaccharomyces pombe*. *Genes Cells* **9**, 671–684.

Chikashige, Y., Tsutsumi, C., Yamane, M., Okamasa, K., Haraguchi, T. & Hiraoka, Y. (2006) Meiotic proteins Bqt1 and Bqt2 tether telomeres to form the bouquet arrangement of chromosomes. *Cell* **125**, 59–69.

Chikashige, Y., Yamane, M., Okamasa, K., Tsutsumi, C., Kojidani, T., Sato, M., Haraguchi, T. & Hiraoka, Y. (2009) Membrane proteins Bqt3 and -4 anchor telomeres to the nuclear envelope to ensure chromosomal bouquet formation. *J. Cell Biol.* **187**, 413–427.

Gonzalez, Y., Saito, A. & Sazer, S. (2012) Fission yeast Lem2 and Man1 perform fundamental functions of the animal cell nuclear lamina. *Nucleus* **3**, 60–76.

Gruenbaum, Y., Margalit, A., Goldman, R.D., Shumaker, D.K. & Wilson, K.L. (2005) The nuclear lamina comes of age. *Nat. Rev. Mol. Cell Biol.* **6**, 21–31.

Grund, S.E., Fischer, T., Cabal, G.G., Antúnez, O., Pérez-Ortín, J.E. & Hurt, E. (2008) The inner nuclear membrane protein Src1 associates with subtelomeric genes and alters their regulated gene expression. *J. Cell Biol.* **182**, 897–910.

Hagan, I. & Yanagida, M. (1995) The product of the spindle formation gene sad1+ associates with the fission yeast spindle pole body and is essential for viability. *J. Cell Biol.* **129**, 1033–1047.

Haraguchi, T., Koujin, T., Segura, M., Lee, K.L., Matsuoka, Y., Yoneda, Y., Wilson, K.L. & Hiraoka, Y. (2001) BAF is required for emerin assembly into the reforming nuclear envelope. *J. Cell Sci.* **114**, 4575–4585.

Harr, J.C., Gonzalez-Sandoval, A. & Gasser, S.M. (2016) Histones and histone modifications in perinuclear chromatin anchoring: from yeast to man. *EMBO Rep.* **17**, 139–155.

Hayles, J., Wood, V., Jeffery, L., Hoe, K.L., Kim, D.U., Park, H.O., Salas-Pino, S., Heichinger, C. & Nurse, P. (2013) A genome-wide resource of cell cycle and cell shape genes of fission yeast. *Open Biol.* **3**, 130053.

Hiraoka, Y. & Dernburg, A.F. (2009) The SUN rises on meiotic chromosome dynamics. *Dev. Cell* **17**, 598–605.

Hiraoka, Y., Maekawa, H., Asakawa, H., Chikashige, Y., Kojidani, T., Osakada, H., Matsuda, A. & Haraguchi, T. (2011) Inner nuclear membrane protein Ima1 is dispensable for intranuclear positioning of centromeres. *Genes Cells* **16**, 1000–1011.

Hou, H., Zhou, Z., Wang, Y., Wang, J., Kallgren, S.P., Kurchuk, T., Miller, E.A., Chang, F. & Jia, S. (2012) Csi1 links centromeres to the nuclear envelope for centromere clustering. *J. Cell Biol.* **199**, 735–744.

Huber, M.D., Guan, T. & Gerace, L. (2009) Overlapping functions of nuclear envelope proteins NET25 (Lem2) and emerin in regulation of extracellular signal-regulated kinase signaling in myoblast differentiation. *Mol. Cell. Biol.* **29**, 5718–5728.

Javerzat, J.P., Cranston, G. & Allshire, R.C. (1996) Fission yeast genes which disrupt mitotic chromosome segregation when overexpressed. *Nucleic Acids Res.* **24**, 4676–4683.

Kawakami, K., Hayashi, A., Nakayama, J. & Murakami, Y. (2012) A novel RNAi protein, Dsh1, assembles RNAi machinery on chromatin to amplify heterochromatic siRNA. *Genes Dev.* **26**, 1811–1824.

Keating, S.T. & El-Osta, A. (2015) Epigenetics and metabolism. *Circ. Res.* **116**, 715–736.

King, M.C., Drivas, T.G. & Blobel, G. (2008) A network of nuclear envelope membrane proteins linking centromeres to microtubules. *Cell* **134**, 427–438.

King, M.C., Lusk, C.P. & Blobel, G. (2006) Karyopherin-mediated import of integral inner nuclear membrane proteins. *Nature* **442**, 1003–1007.

Korfali, N., Wilkie, G.S., Swanson, S.K., Srsen, V., de Las Heras, J., Batrakou, D.G., Malik, P., Zuleger, N., Kerr, A.R., Florens, L. & Schirmer, E.C. (2012) The nuclear envelope proteome differs notably between tissues. *Nucleus* **3**, 552–564.

Laguri, C., Gilquin, B., Wolff, N., Romi-Lebrun, R., Courchay, K., Callebaut, I., Worman, H.J. & Zinn-Justin, S. (2001) Structural characterization of the LEM motif common to three human inner nuclear membrane proteins. *Structure* **9**, 503–511.

Lee, K.K., Haraguchi, T., Lee, R.S., Koujin, T., Hiraoka, Y. & Wilson, K.L. (2001) Distinct functional domains in emerin bind lamin A and DNA-bridging protein BAF. *J. Cell Sci.* **114**, 4567–4573.

Lee, K.K. & Wilson, K.L. (2004) All in the family: evidence for four new LEM-domain proteins Lem2 (NET-25), Lem3, Lem4 and Lem5 in the human genome. *Symp. Soc. Exp. Biol.* **56**, 329–339.

Lee, M.S. & Craigie, R. (1998) A previously unidentified host protein protects retroviral DNA from autointegration. *Proc. Natl Acad. Sci. USA* **95**, 1528–1533.

Lin, F., Blake, D.L., Callebaut, I., Skerjanc, I.S., Holmer, L., McBurney, M.W., Paulin-Levasseur, M. & Worman, H.J. (2000) MAN1, an inner nuclear membrane protein that shares the LEM domain with lamina-associated polypeptide 2 and emerin. *J. Biol. Chem.* **275**, 4840–4847.

Liu, J., Lee, K.K., Segura-Totten, M., Neufeld, E., Wilson, K.L. & Gruenbaum, Y. (2003) MAN1 and emerin have overlapping function(s) essential for chromosome segregation and cell division in *Caenorhabditis elegans*. *Proc. Natl Acad. Sci. USA* **100**, 4598–4603.

Malone, C.J., Fixsen, W.D., Horvitz, H.R. & Han, M. (1999) UNC-84 localizes to the nuclear envelope and is required for nuclear migration and anchoring during *C. elegans* development. *Development* **126**, 3171–3181.

Mans, B.J., Anantharaman, V., Aravind, L. & Koonin, E.V. (2004) Comparative genomics, evolution and origins of the nuclear envelope and nuclear pore complex. *Cell Cycle* **3**, 1612–1637.

Matsumoto, T., Fukui, K., Niwa, O., Sugawara, N., Szostak, J.W. & Yanagida, M. (1987) Identification of healed terminal DNA fragments in linear minichromosomes of *Schizosaccharomyces pombe*. *Mol. Cell. Biol.* **7**, 4424–4430.

Meier, J.L. (2013) Metabolic mechanisms of epigenetic regulation. *ACS Chem. Biol.* **8**, 2607–2621.

Mekhail, K. & Moazed, D. (2010) The nuclear envelope in genome organization, expression and stability. *Nat. Rev. Mol. Cell Biol.* **11**, 317–328.

Moreno, S., Klar, A. & Nurse, P. (1991) Molecular genetic analysis of fission yeast *Schizosaccharomyces pombe*. *Methods Enzymol.* **194**, 795–823.

Sato, M., Dhut, S. & Toda, T. (2005) New drug-resistant cassettes for gene disruption and epitope tagging in *Schizosaccharomyces pombe*. *Yeast* **22**, 583–591.

Schindelin, J., Arganda-Carreras, I., Frise, E. *et al.* (2012) Fiji: an open-source platform for biological-image analysis. *Nat. Methods* **9**, 676–682.

Schirmer, E.C., Florens, L., Guan, T., Yates, J.R. 3rd & Gerace, L. (2003) Nuclear membrane proteins with potential disease links found by subtractive proteomics. *Science* **301**, 1380–1382.

Schirmer, E.C. & Gerace, L. (2005) The nuclear membrane proteome: extending the envelope. *Trends Biochem. Sci.* **30**, 551–558.

Shumaker, D.K., Lee, K.K., Tanhehco, Y.C., Craigie, R. & Wilson, K.L. (2001) LAP2 binds to BAF.DNA complexes: requirement for the LEM domain and modulation by variable regions. *EMBO J.* **20**, 1754–1764.

Spitz, F., Gonzalez, F. & Duboule, D. (2003) A global control region defines a chromosomal regulatory landscape containing the HoxD cluster. *Cell* **113**, 405–417.

Steglich, B., Filion, G.J., van Steensel, B. & Ekwall, K. (2012) The inner nuclear membrane proteins Man1 and Ima1 link to two different types of chromatin at the nuclear periphery in *S. pombe*. *Nucleus* **3**, 77–87.

Takayama, Y., Sato, H., Saitoh, S., Ogiyama, Y., Masuda, F. & Takahashi, K. (2008) Biphasic incorporation of centromeric histone CENP-A in fission yeast. *Mol. Biol. Cell* **19**, 682–690.

Tange, Y. & Niwa, O. (2008) *Schizosaccharomyces pombe* Bub3 is dispensable for mitotic arrest following perturbed spindle formation. *Genetics* **179**, 785–792.

Towbin, B.D., Gonzalez-Sandoval, A. & Gasser, S.M. (2013) Mechanisms of heterochromatin subnuclear localization. *Trends Biochem. Sci.* **38**, 356–363.

Tzur, Y.B., Wilson, K.L. & Gruenbaum, Y. (2006) SUN-domain proteins: 'Velcro' that links the nucleoskeleton to the cytoskeleton. *Nat. Rev. Mol. Cell Biol.* **7**, 782–788.

Ulbert, S., Antonin, W., Platani, M. & Mattaj, I.W. (2006) The inner nuclear membrane protein Lem2 is critical for normal nuclear envelope morphology. *FEBS Lett.* **580**, 6435–6441.

Van de Vosse, D.W., Wan, Y., Wozniak, R.W. & Aitchison, J.D. (2011) Role of the nuclear envelope in genome organization and gene expression. *Wiley Interdiscip. Rev. Syst. Biol. Med.* **3**, 147–166.

Wach, A. (1996) PCR-synthesis of marker cassettes with long flanking homology regions for gene disruptions in *S. cerevisiae*. *Yeast* **12**, 259–265.

Wagner, N. & Krohne, G. (2007) LEM-Domain proteins: new insights into lamin-interacting proteins. *Int. Rev. Cytol.* **261**, 1–46.

Worman, H.J. & Schirmer, E.C. (2015) Nuclear membrane diversity: underlying tissue-specific pathologies in disease? *Curr. Opin. Cell Biol.* **34**, 101–112.

Xu, Y.J. (2016) Inner nuclear membrane protein Lem2 facilitates Rad3-mediated checkpoint signaling under replication stress induced by nucleotide depletion in fission yeast. *Cell. Signal.* **28**, 235–245.

Yorifuji, H., Tadano, Y., Tsuchiya, Y., Ogawa, M., Goto, K., Umetani, A., Asaka, Y. & Arahata, K. (1997) Emerin, deficiency of which causes Emery-Dreifuss muscular dystrophy, is localized at the inner nuclear membrane. *Neurogenetics* **1**, 135–140.

Zaratiegui, M., Vaughn, M.W., Irvine, D.V., Goto, D., Watt, S., Bähler, J., Arcangioli, B. & Martienssen, R.A. (2011) CENP-B preserves genome integrity at replication forks paused by retrotransposon LTR. *Nature* **469**, 112–115.

Received: 16 March 2016
Accepted: 8 May 2016

Supporting Information

Additional Supporting Information may be found online in the supporting information tab for this article:

Table S1 List of strains used

Table S2 List of primers used for ChIP assay